5-2018

Fossil Moles from the Gray Fossil Site, TN: Implications for Diversification and Evolution of North American Talpidae

Danielle Oberg
East Tennessee State University

Fossil Moles from the Gray Fossil Site, TN: Implications for Diversification and Evolution of North American Talpidae

---

A thesis
presented to
the faculty of the Department of Geosciences
East Tennessee State University

In partial fulfillment
of the requirements for the degree
Master of Science in Geology

---

by
Danielle E. Oberg
May 2018

Joshua X. Samuels, PhD, Chair
Blaine W. Schubert, PhD
Christopher C. Widga, PhD

Keywords: Talpidae, Gray Fossil Site, Systematics, Morphometrics, Cluster Analysis

ABSTRACT

Fossil Moles from the Gray Fossil Site, TN: Implications for Diversification and Evolution of North American Talpidae

by

Danielle E. Oberg

The Gray Fossil Site (GFS) is one of the richest Cenozoic terrestrial localities in the eastern United States. This study describes the first talpid specimens recovered from the GFS. Using measurements and comparisons of dental and humerus morphology, I identify 4 talpids (*Parascalops* nov. sp., *Quyania* cf. *Q. europaea*, *Mioscalops* (= *Scalopoides*) sp., and an unidentified stem desman) occurring at the GFS. Humeral morphology has been used to diagnose talpid species and study relationships. A geometric morphometric analysis showed that humerus shape is highly reflective of locomotor ecology in extant talpids and allows ecological inferences for fossil talpids. Hierarchical cluster analysis using morphometric data allowed examination of similarity among taxa and helped to secondarily verify taxonomic designations for the GFS taxa. The resulting phenogram showed strong similarity to the most up-to-date molecular cladogram and actually matched phylogenetic relationships substantially better than any morphological cladistic analyses to date.

ACKNOWLEDGMENTS

I would like to thank my chair, Dr. Josh Samuels, as well as my other committee members, Dr. Chris Widga and Dr. Blaine Schubert, for their guidance and support throughout this project. I also want to thank Shawn Haugrud for leading the field excavations that resulted in me having this bountiful material to work on, the dedicated group of volunteers that picked through thousands of pounds of sediment to find this material, April Nye for cataloguing and housing all of this material in the East Tennessee State University (ETSU) fossil collections, Keila Bredehoeft for repairing all the fossils I broke, Brian Compton for access to the ETSU modern mammal collection, and the Los Angeles County Museum of Natural History and the Smithsonian Museum of Natural History for allowing me access to their modern mammal collections. I would also like to thank the Don Sundquits Center for Excellence in Paleontology for funding me during my time at ETSU and NSF for funding the excavations that yielded the fossil material utilized in this study. Additionally, I would like to thank my fellow graduate students, past and current, and the Gray Fossil Site Museum staff and volunteers for all of their support and encouragement while attending ETSU. Finally, I would like to thank Max and Mr. Josie, my two beautiful cats, for all of their emotional support throughout my graduate career.

TABLE OF CONTENTS

Page

LIST OF TABLES

LIST OF FIGURES

Figure Page

CHAPTER 1

INTRODUCTION

Talpidae (true moles, shrew moles, and desmans) is an ecologically diverse family that is widely distributed across the northern hemisphere (Nowak and Paradiso 1983; Gorman and Stone 1990; Gunnell et al. 2008). Talpids are well known for their subterranean lifestyles and unique morphological modifications for fossorial specialization (Freeman 1886; Campbell 1939; Reed 1951; Yalden 1966; Gorman and Stone 1990; Sánchez-Villagra et al. 2004; Meier et al. 2013); however, semi-aquatic and terrestrial locomotor ecologies are also common (Nowak and Paradiso 1983; Gorman and Stone 1990). Even though there are variable locomotor ecologies among extant talpids, convergent evolution strongly influences body shape, creating problems for researchers interested in understanding the evolutionary history and diversification of the family.

Convergent evolution among specialized clades has created major discrepancies between talpid molecular and morphological phylogenies (Douady et al. 2002; Symonds 2005; Sánchez-Villagra et al. 2006; He et al. 2016). Similar morphology makes it difficult to choose morphological characters independent of ecology and most molecular studies lack confidence on cluster positions. To better understand the source of some of the discrepancies, I am using 2D geometric morphometrics of humeri to determine how morphology reflects ecology, and thus evaluate phylogenetically informative morphological features. Previous studies (Rohlf et al. 1996; Piras et al. 2012; Sansalone et al. 2015) have shown that geometric morphometrics can be useful for assessing relationships in talpids.

The fossil record for Talpidae is relatively well-known; the oldest members of the family are from the Eocene of Asia (Gorman and Stone 1990) and peak diversity occurred during the

Miocene of both Eurasia and North America (Gunnell et al. 2008). Though talpids in North America are discussed by Gunnell et al. (2008), there has yet to be a detailed review of the family, and thus, relatively little is known about the diversification of, and relationships between, North American talpid species. I am using new talpid occurrences from the Gray Fossil Site to fill in gaps in the North American fossil record, look at dispersal patterns between Eurasia and North America, and understand talpid evolution during the Cenozoic.

Background

Talpidae is an ecologically diverse family consisting of: terrestrial shrew moles, semi-fossorial shrew moles, semi-aquatic desmans, as well as semi-fossorial and fossorial moles (Koyabu et al. 2011). Currently, the most parsimonious phylogenetic hypothesis comes from He et al. (2016) (Figure 1). There are six recognizable clades representing the 7 major tribes and 1 subfamily: Uropsilinae (Chinese terrestrial shrew moles), Scalopini (North American/Asian fossorial moles), Scaptonychini (Chinese fossorial long-tailed moles), Urotrichini (Japanese semi-fossorial shrew moles), Neurotrichini (North American semi-fossorial shrew moles), Condylurini (North American semi-fossorial star-nosed mole), Desmanini (Eurasian semi-aquatic desmans), and Talpini (Eurasian fossorial moles). Though the Scaptonychini tribe does not contain any shrew moles, it is most similar both molecularly and morphologically to the extant shrew mole groups. Two of the six clusters are exclusively fossorial: the Eurasian Talpini and North American/Asian Scalopini. It is hypothesized that these two clusters convergently evolved similar derived morphological fossorial specializations (Gorman and Stone 1990; Piras et al. 2012; Meier et al. 2013; He et al. 2016).

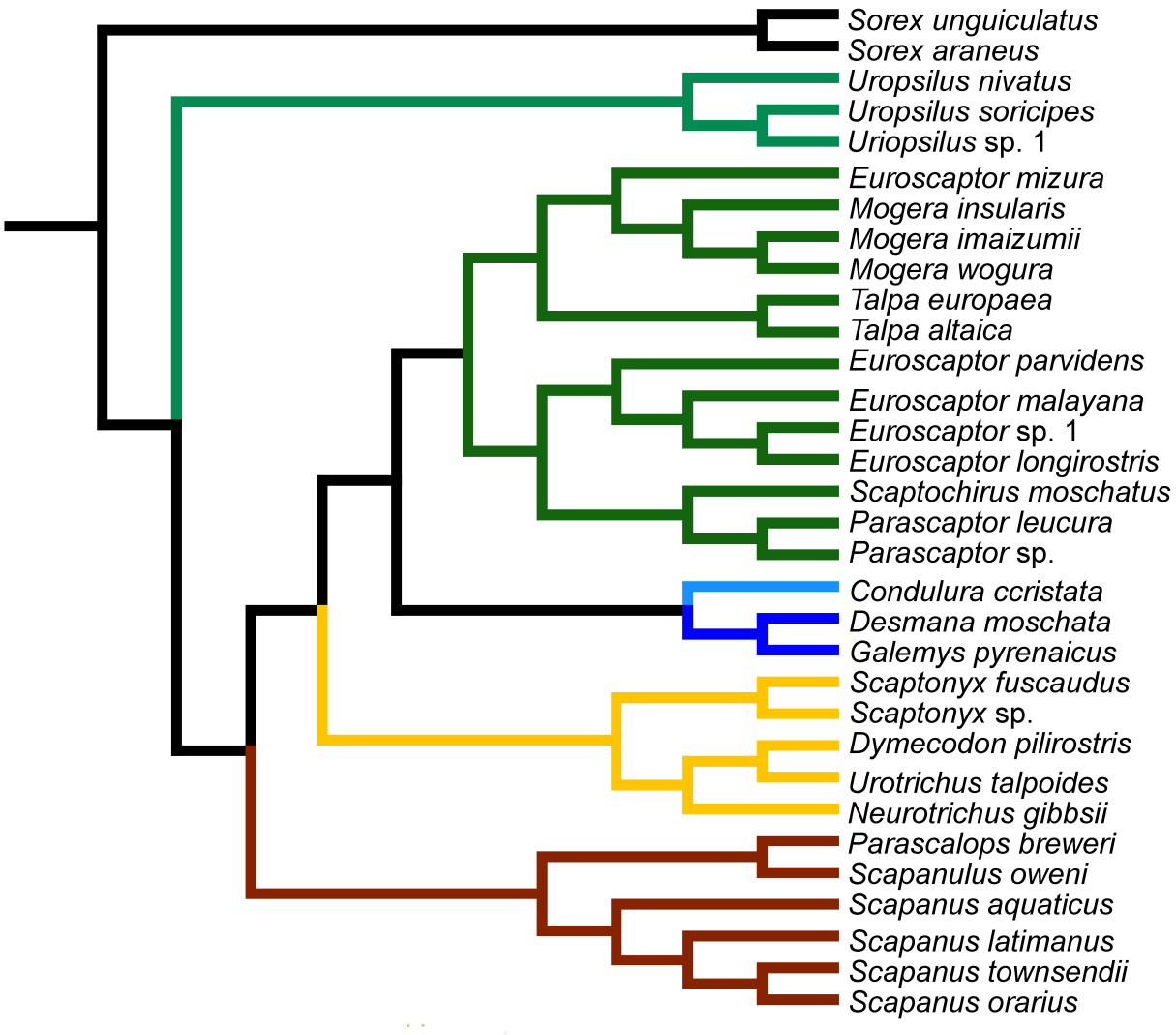

Figure 1: Phylogeny of Talpidae, modified from He et al. (2016) color-coded to match the current tribes and subfamilies. Outgroup: Soricidae (black) – Shrews. Talpidae: Uropsilinae (light green) – Chinese terrestrial shrew moles; Scalopini (brown) – North American/Asian fossorial moles; Scaptonychini (yellow) – Chinese semi-fossorial moles; Urotrichini (yellow) – Japanese and North American semi-fossorial shrew moles; Neurotrichini (yellow) – North American semi-fossorial shrew moles; Condylurini (light blue) – North American semi-fossorial moles; Desmanini (dark blue) – Eurasian semi-aquatic desmans; Talpini (dark green) – Eurasian fossorial moles.

Ancestors to talpids are hypothesized to be fully terrestrial. Sometime before or during the Eocene, there would have been a transformation from a terrestrial to a fossorial life style (Sánchez-Villagra et al. 2004), which resulted in the humerus of fossorial moles becoming extremely short, broad, and compact, with pronounced muscle attachments (Yalden 1966; Hildebrand 1974; Whidden 2000; Gambaryan et al. 2002; Meier et al. 2013). Additionally, both proximal and distal ends are positioned in opposite directions, which relates to mid-shaft torsion (Freeman 1886; Whidden 2000). This humeral morphology is only found in talpids (Reed 1951; Yalden 1966; Sánchez-Villagra et al. 2004; Meier et al. 2013) and several studies (Gambaryan et al. 2002; Meier et al. 2013) have shown this morphology is most likely related to the expansion of muscle attachment sites.

All extant fossorial talpids move their forearms using humeral rotation. This type of humerus movement is exclusive to the family Talpidae (Reed 1951; Yalden 1966; Sánchez-Villagra et al. 2004; Meier et al. 2013). The humerus is permanently abducted, the elbow joint flexed and the hand in a plane perpendicular to the axis of rotation of the humerus (Yalden 1966; Thewissen and Badoux 1986). The power stroke originates from contracting the *M. teres major*, *pectoralis transversus*, *latissimus dorsi* and *suscapularis* causing the humerus to rotate outwards, humeral rotation pulls the hand caudally (Yalden 1966). This mode of digging works best in moderately soft soils (Hildebrand 1974).

Forelimb robustness increases the likelihood of humeri being preserved, but can also provide insights into locomotor adaptations through time. However, the resolution of locomotor adaptations through time requires a well-resolved phylogeny. Numerous phylogenetic hypotheses have been proposed based on osteological, myological, and molecular data (Hutchison 1976; Yates and Moore 1990; Whidden 2000; Motokawa 2004; Shinohara et al.

2004; Cabria et al. 2006; Sanchez-Villagra et al. 2006; Bannikova et al. 2015; Schwermann and Thompson 2015), but often they reveal more conflicts than resolve the problem. This creates additional problems regarding the establishment and composition of subfamilies and tribes (Hutchison 1968; Yates 1984; McKenna and Bell 1997; Hutterer 2005), with substantial confusion surrounding the phylogenetic placement and taxonomic assignment of fossil forms (Ziegler 2003; 2012; Klietmann et al. 2015; He et al. 2016). Recent work by He et al. (2016) has produced a molecular based phylogeny with strong statistical support for each cluster. I am using this phylogeny as my comparative phylogeny for the remainder of this project.

In comparison to many other mammalian families, relatively little work has been done to understand the evolutionary history of the family Talpidae. The study of Talpidae, and all its decedents, was popular in the 1930s and 1940s (Hamilton 1931; Campbell 1939; Eadie 1939; Schreuder 1940; Dalquest and Orcutt 1942). New interest began in the 1960s with J. H. Hutchinson's work on fossil talpids from Oregon (Hutchison 1968; 1974; 1984; 1987). More research into talpid evolutionary history occurred in the 1990s and early 2000s as the scientific community had access to more tools to study actual phylogenetic relationships and examine convergent morphology between taxa (Gorman and Stone 1990; Yates and Moore 1990; Rohlf, Loy, and Corti 1996; Whidden 2000; Motokawa 2004; Sánchez-Villagra et al. 2004; Shinohara et al. 2004; Symonds 2005; Sánchez-Villagra et al. 2006).

Geologic Setting

The Gray Fossil Site (GFS) is a latest Miocene or earliest Pliocene, either latest Hemphillian or earliest Blancan North American Land Mammal Age (NALMA), site in northeastern Tennessee. Age of the GFS is between 7 and 4.5 Ma, based on the stratigraphic ranges of the rhino *Teleoceras* and ursid *Plionarctos* (Wallace and Wang 2004). The geology

includes multiple karst sub-basins that filled with lacustrine sediments (Shunk et al. 2006; Whitelaw et al. 2008; Shunk et al. 2009), which indicates that the GFS was once a limestone paleosinkhole that filled in and became a 40 m-deep paleosinkhole lake (Shunk et al. 2006; 2009; Zobaa et al. 2011). The stratigraphy consists of thin layers of locally derived silts and sands with low organic content overlain by thin layers of organic matter with alternating bands of quartz sand and carbonate silt (Shunk et al. 2006; 2009).

Numerous vertebrate taxa as well as abundant plant fossils (Wallace and Wang 2004; Worobiec et al. 2011; Zobaa et al. 2011; Mead et al. 2012; Ochoa et al. 2012; 2016) indicate that there was a dense forest surrounding the paleosinkhole lake. The lake was a year-round water source supported the presence of fossil fish, neotenic salamanders, aquatic turtles, alligators, and beavers (Parmalee et al. 2002; Boardman and Schubert 2011; Mead et al. 2012; Jasinski 2013; Bourque & Schubert 2015). The plants suggest that the flora was predominantly arboreal, which resembles what is currently found in lower elevations of the southern Appalachians (Wallace and Wang 2004; Gong et al. 2010). The floras also indicate strong Asian influences (Gong et al. 2010), and the presence of humid, wetland areas (Brandon 2013; Worobiec et al. 2013). Carbon and oxygen isotopic analyses from GFS ungulate teeth suggest a dense forest around the lake and climate with little seasonal temperature and precipitation variation (DeSantis & Wallace 2008).

CHAPTER 2

METHODS

Morphological comparisons of extant and extinct talpid taxa, supplemented with linear measurements, were used to determine taxonomic identifications for the Gray Fossil Site talpid material. I examined dental material (n=152 maxillae and n=69 mandibles) and postcrania (n=135 humeri) from all 17 extant talpid genera (*Condylura* n=19, *Desmana* n=2, *Dymecodon* n=2, *Euroscaptor* n=3, *Galemys* n=3, *Mogera* n=3, *Neurotrichus* n=15, *Parascalops* n=10, *Parascaptor* n=1, *Scalopus* n=25, *Scapanulus* n=3, *Scapanus* n=13, *Scaptochirus* n=2, *Scaptonyx* n=3, *Talpa* n=3, *Uropsilus* n=6, and *Urotrichus* n=2), along with 21 extinct species for morphological comparisons. I did not examine any postcranial material for *Desmana* or *Parascaptor*. Extant material came from the Smithsonian Museum of Natural History (NMNH), the Los Angeles County Museum of Natural History (LACM), the East Tennessee State University comparative osteology collection (ETVP), and published literature sources. Fossil material came from the published literature and the East Tennessee State University Museum of Natural History (ETMNH).

Extant specimens were photographed in standard diagnostic views (dental – lingual, labial, and occlusal; postcrania – anterior, posterior, and lateral). All material was photographed using either a Canon Rebel Ti DSLR camera with a macro lens attached to a copy stand or a Dino-Lite Edge MZ4815 digital microscope camera using the associated DinoCapture 2.0 software version 1.5.27.A. Linear measurements (Figure 2) were performed based on photographs analyzed in ImageJ (Schneider et al. 2012).

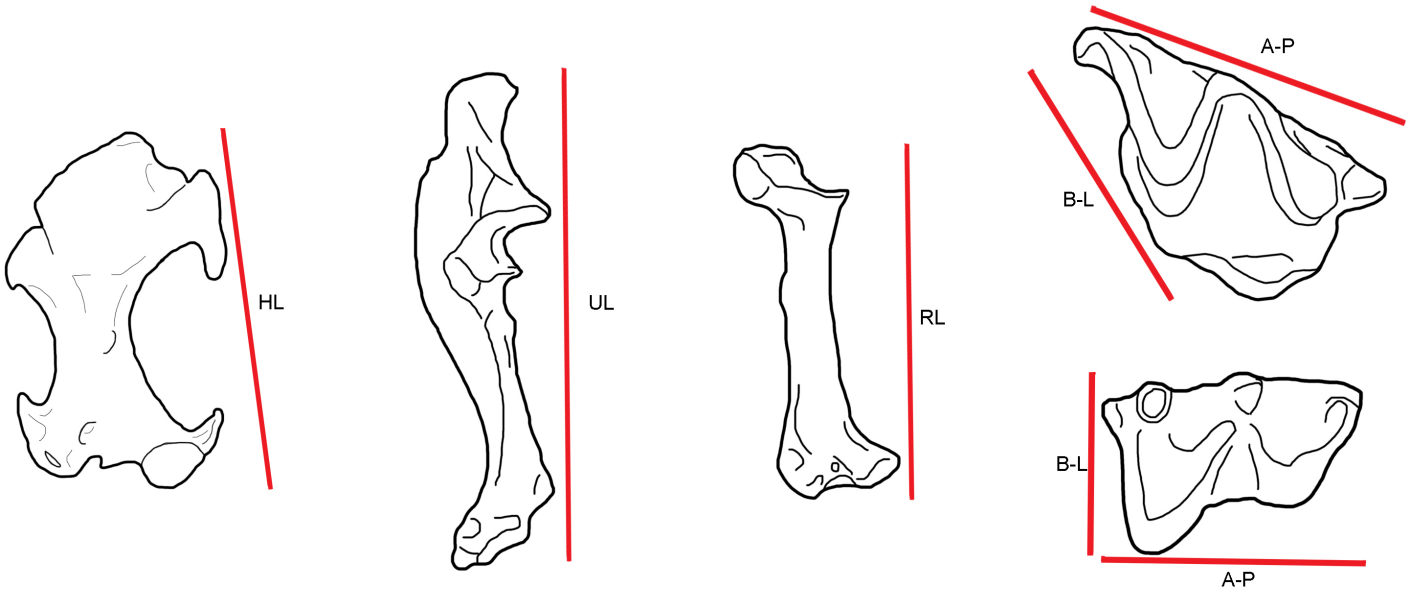

Figure 2: Linear measurements used for morphological comparison. HL – total humerus length; proximal-most tip of greater tuberosity to distal-most point on capitulum. UL – total ulna length; proximal-most tip of olecranon process to distal-most tip of terminal process. RL – total radius length: proximal-most tip of capitular process to distal-most tip of lunar articular facet. B-L – buccolingual width; upper teeth – posterior-most tip of the metastyle to the lingual margin of the protocone; lower teeth – lingual-most tip of the metaconid to the buccal margin of the talonid. A-P – anteroposterior length; upper teeth – posterior-most tip of the metastyle to the anterior-most tip of the parastyle; lower teeth – anterior tip of the trigonid (paraconid) to the posterior end of the talonid (entostylid).

I also performed a 2D geometric morphometric analysis by digitizing 24 landmarks onto 135 humeri (*Condylura* n=16, *Dymecodon* n=1, *Euroscaptor* n=3, *Galemys* n=3, *Mogera* n=3, *Neurotrichus* n=15, *Parascalops* n=6, *Scalopus* n=22, *Scapanulus* n=1, *Scapanus* n=13, *Scaptochirus* n=2, *Scaptonyx* n=1, *Talpa* n=3, *Uropsilus* n=6, *Urotrichus* n=1, and fossils n=27), representing 42 taxa. I used the TPS Software series by SUNY Stony Brook to do the geometric

morphometrics analyses (Rohlf 2006). Landmarks (Figure 3, Table 1) were chosen, and modified, from previous studies (Piras et al. 2012; Sansalone et al. 2015). Only one view (anterior) was used to maximize the number of taxa that could be included in the analysis.

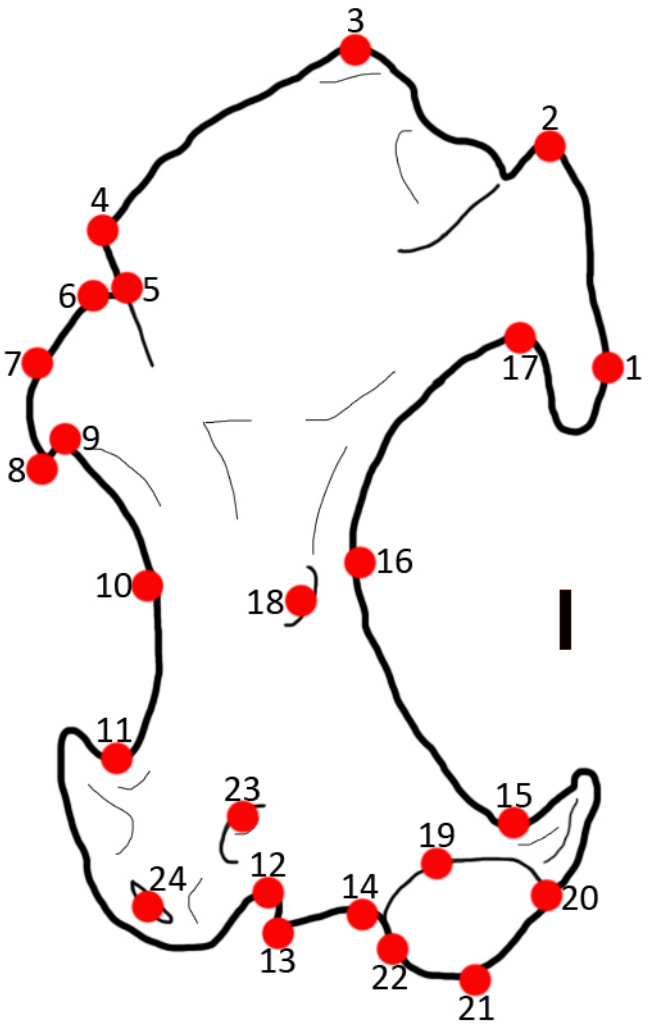

Figure 3: Number and position of humerus landmarks. Line drawing showing landmarks positions with labels on the anterior view of a left humerus of *Condylura cristata* (Star-nosed mole). Scale bar = 1 mm.

Table 1: Numbers and Descriptions of All Landmarks. Directionality of character naming reflects orientation in Figure 3. Characters labeled and named according to Hutchison (1968).

Landmark	Description
1	Distal end of lesser tuberosity
2	Proximal end of lesser tuberosity
3	Proximal end of greater tuberosity
4	Distal end of greater tuberosity
5	Inflection between greater tuberosity and teres tubercle
6	Proximal end of teres tubercle
7	Greatest point of curvature on teres tubercle
8	Distal end of teres tubercle
9	Inflection between teres tubercle and minor sulcus
10	Greatest point of curvature of minor sulcus
11	Inflection between minor sulcus and entepicondylar process
12	Inflection between *M. flexor digitorum* ligament and trochlea
13	Lateral aspect of trochlea
14	Medial aspect of trochlea
15	Inflection between capitulum and major sulcus
16	Greatest point of curvature of major sulcus
17	Inflection between major sulcus and greater tubercle
18	Pectoral tubercle
19	Superior aspect of capitulum
20	Medial aspect of capitulum
21	Inferior aspect of capitulum
22	Lateral aspect of capitulum
23	Entepicondylar foramen
24	Fossa of the *M. flexor digitorum* ligament

I performed a relative warps analysis using the geometric morphometric landmark data to examine variation in humerus shape among taxa. Partial warp scores, uniform components, and relative warp scores were saved for subsequent analyses in SPSS 24 (IBM Corp. 2013). I ran a canonical variate analysis (CVA) in SPSS using partial warp scores and uniform components to examine how humeral morphology was related to locomotor ecology. Locomotor ecologies

(Table 2) were derived from literature sources and all extant taxa were categorized into one of four groups. Fossil taxa were included as unknowns to be classified by the analysis. A hierarchical cluster analysis (using the UPGMA clustering method with squared Euclidian distance), was conducted using partial warp scores and uniform components as variables and was used to examine morphological similarity of taxa. Variables in the CVA with a correlation coefficient greater than 0.3 were considered functionally-linked and excluded from the cluster analysis. The cluster analysis results were input into Mesquite (Maddison and Maddison 2018) to visualize change in continuous and categorical variables across the dendrogram.

Table 2: Defining Locomotor Categories. Locomotor categories used in this study and their definitions modified from Polly (2007).

Locomotor category	Description
Terrestrial	Spends most of time foraging on ground. May maintain a burrow for sleeping.
Semi-aquatic	Spends most of time foraging in water. May maintain a burrow for sleeping.
Semi-fossorial	Spends time foraging underground and on the surface.
Fossorial	Fully subterranean lifestyle.

Two cluster analysis dendrograms were generated: one using all individuals and the other using species means. The dendrogram depicting individuals was used to see how well pre-existing clusters could be recreated. The species means dendrogram shows the average position for each taxon, and was used for comparison against the most up-to-date molecular phylogeny by He et al. (2016) to evaluate goodness-of-fit as well as for ancestral state reconstructions across the family.

Ancestral state reconstructions were done to test hypotheses about changes in body size, biogeography, and ecology through time. All reconstructions were done using squared change parsimony in Mesquite. One reconstruction was done using humerus length (Figure 2) as a proxy for body size to see how body size changed through time. Another was done using the CVA scores, which reflect locomotor ecology, to evaluate how locomotor specializations changed across linages. A third was performed using spatial data from the published literature to test biogeographical hypotheses.

I examined global talpid dispersion patterns through the Cenozoic using occurrence data from the NOW database (Fortelius 2013; http://pantodon.science.helsinki.fi/now/), NEOTOMA databases (FAUNMAP and MIOMAP (Carrasco et al. 2007; Graham and Lundelius 2010; http://www.ucmp.berkeley.edu/neomap/)), and a variety of literature sources. Maps were created in QGIS version 2.18.

CHAPTER 3

SYSTEMATIC PALEONTOLOGY

Class MAMMALIA Linnaeus, 1758

Order EULIPOTYPHLA Haeckel, 1866

Family TALPIDAE Fischer von Waldhelm, 1814

Subfamily TALPINAE Fischer von Waldhelm, 1814

Tribe DESMANINI? Thomas, 1912

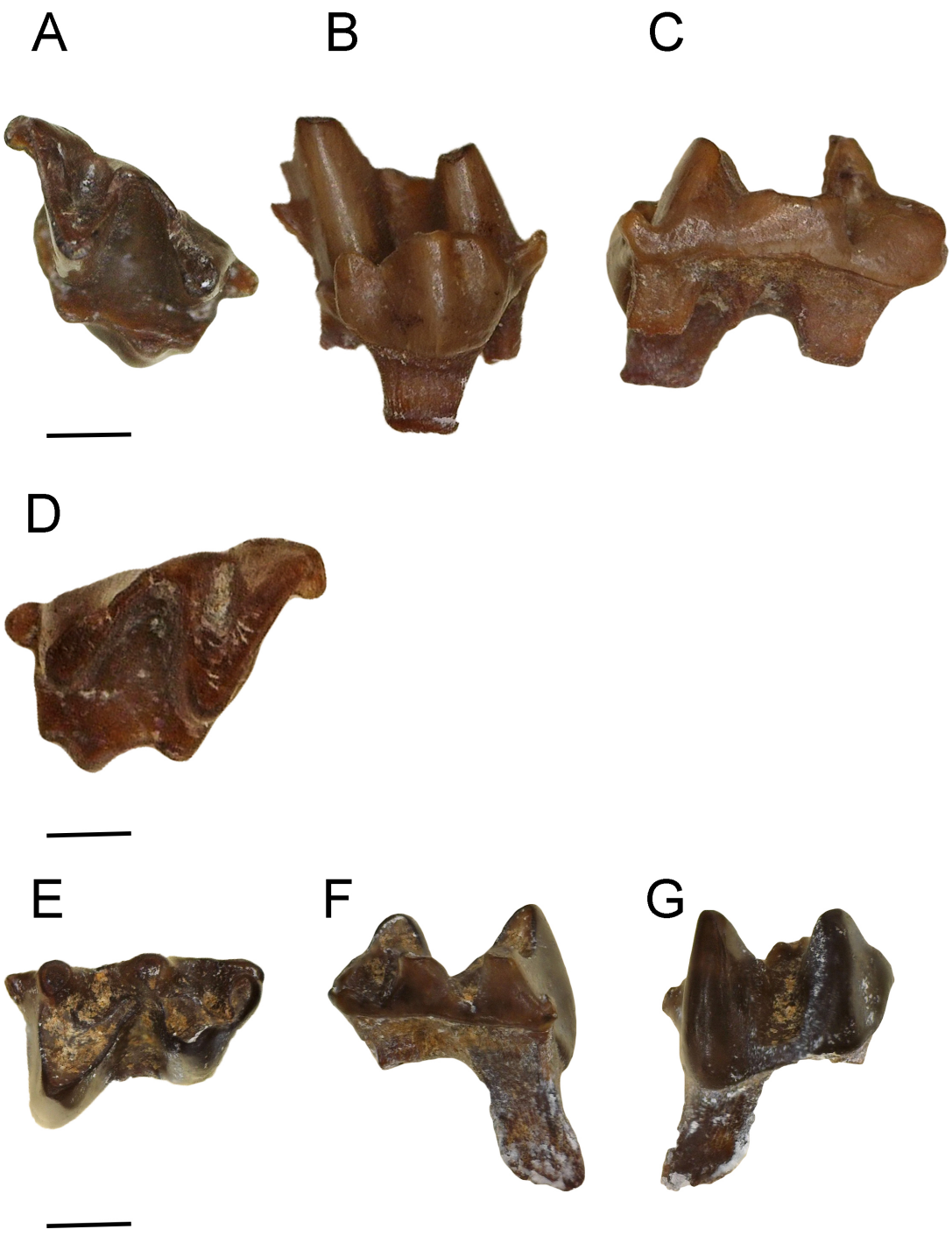

Figure 4: Desman dental material. Right M1. ETMNH 20779 A) occlusal, B) lingual, and C) labial views. Left M1. ETMNH 20747 D) occlusal view. Right m2. ETMNH 9664 E) occlusal, F) labial, and G) lingual views. Scale bars = 1 mm.

Referred specimens – ETMNH 20747 - left M1; ETMNH 20779 - right M1; ETMNH 9664 - right m2.

Locality – Gray Fossil Site, TN.

Diagnosis – Large size; anteroposteriorly elongated lower molar; m2 lacking anterior, posterior, and lingual cingulids; m2 cristid obliqua joins metaconid; upper molars with continuous mesostyle; M1 lingual border with distinct, lingually projecting, protoconule and metaconule, either larger than or equal in size to the protocone.

Description – ETMNH 20747 and 20779 both resemble a typical talpid M1, but are large (Figure 4). They have a lopsided triangular outline due to the great difference in the morphology of the labial cusps and have pre- and post- cingula. The paracone and metacone are crescentic in shape and relatively similar in size, but the paracone is slightly smaller. The protocone is also large and centrally placed. The teeth are very open; the paracone and metacone are well separated. There is a large paraconule about the same size as the paracone. The mesostyle is not divided. The protoconule and the metaconule are well-developed and influence the lingual outline of the crown causing the antero- and posterolingual side to bulge outwards. The protoconule is closely appressed to the anterior margin of the protocone. A deep basin lies between the protocone, paracone, and metacone.

ETMNH 9664 is a very large tooth for a talpid (Figure 4). The cusps are relatively worn. The talonid is about the same length as the trigonid, but substantially wider. The entire tooth is anterioposteriorly elongated. The talonid and trigonid are both very open. There is a large reentrant valley between the trigonid and talonid. The cristid obliqua joins with the metaconid. There are no anterior, posterior, or lingual cingulids. The paraconid, metaconid, and

entoconid are much lower than protoconid and hypoconid. The metaconid and entoconid are about the same size, but the metaconid is a little bit larger. The entoconid shows signs of heavy wear. The entostylid is large and triangular. The paraconid has an extra bladed notch along the posterior aspect.

Discussion – The formal systematic classification of desmans has been debated for quite some time. This group was previously classified as a subfamily (Barabasch-Nikiforow 1975; Hutchison 1974; Rümke 1985) called Desmaninae. Some researchers thought there was enough morphological distinction between desmans and other talpids to warrant a family-level designation; however, recent genetic work (Shinohara et al. 2003; Shinohara et al. 2004; He et al. 2014; He et al. 2016) shows that this group falls within the subfamily Talpinae and should be classified as a tribe.

The morphology and size of these three molars are reminiscent of extant desmans, but these teeth do not represent either of the two extant genera. The ETMNH specimens are comparable in size to *Desmana* (Russian desman), but are larger than *Galemys* (Pyrenees desman) (Table 3). The M1 of extant desmans resembles that of other talpids in occlusal shape and generalized morphology. However, extant desman upper molars always have a divided mesostyle (also referred to as distinctly twinned mesostyle) and a strongly developed lingual part featuring a protoconule, a protocone, a metaconule and often a small tubercle on the posterocrista of the protocone (Miller 1912; Schreuder 1940; Saban 1958; Hugueney 1972; Rümke 1985). These cuspules act like additional cusps and increase the food processing surface area on the tooth, aiding in efficient food processing (Rümke 1985).

Table 3: Desman Tooth Size Comparisons. A-P is anteroposterior length. B-L is buccolingual width. Ranges and measurements in mm. The ranges for *Archaeodesmana* include all 9 accepted species (*A. pontica* Schreuder 1940, *A. vinea* Storch, 1978, *A. turolensis* Rümke, 1985, *A. adroveri* Rümke, 1985, *A. luteyni* Rümke, 1985, *A. major* Rümke, 1985, *A. dekkersi* Rümke, 1985, *A. brailloni* Rümke, 1985 and *A. bifida* Engesser, 1980).

Taxon	M1		m2	
	A-P	B-L	A-P	B-L
Desmana moschata (n = 8)	2.95 – 4.60	2.55 – 4.70	2.25 – 4.00	3.00 – 3.32 (n = 3)
Galemys pyrenaicus (n = 12)	2.35 – 3.30	2.20 – 3.39	2.20 – 2.95	1.18 – 2.11 (n = 8)
Archaeodesmana† (Martín-Suárez et al., 2001)	2.60 – 3.50	2.00 – 3.10	2.10 – 2.70	--
Lemoynea biradicularis† (Bown, 1980)	2.71 – 2.72	2.92 – 3.08	2.17 – 2.28	1.56 – 1.75
ETMNH 20747	3.41	3.35	-	-
ETMNH 20779	3.57	3.43	-	-
ETMNH 6994	-	-	2.98	2.37

An important feature that has been used as an apomorphy for defining the tribe Desmanini is the cristid obliqua of the lower molars ends either 1) against the tip of the metaconid, or 2) against the protoconid-metaconid crest (Miller 1912; Schreuder 1940; Saban 1958; Hugueney 1972; Rümke 1985). Specifically looking at the m2, a strong entostylid is always present in extant desmans. It can be either a bulge formed by the posterior cingulum or a rounded or elliptical tubercle situated near the enamel-dentine boundary. The shape and size of the cusps, as well as the position of cristid obliqua are highly variable. The teeth can be heavy with sturdy obtuse cusps and high connecting ridges, or more slender with sharp cusps and low crests. The cristid obliqua may be short or long, ending either against the protoconid-metaconid crest or near the tip of the metaconid (Rümke 1985).

The teeth of extant desmans are most morphologically similar to extant shrew moles, but are larger (Schreuder 1940; Rümke 1985). In lower molars, the talonid is v-shaped like all talpids, not u-shaped like soricids. In the upper molars, accessory cuspules along the lingual boarder in desmans functions like the hypocone in shrew moles (Schreuder 1940; Palmeirim and Hoffmann 1983; Carraway and Verts 1991). The cusps on upper and lower molars tend to be low-crowned, when compared to other extant talpids, and more bulbous because the diet of extant desmans consists of benthic invertebrates (Palmeirim and Hoffmann 1983; Rümke 1985).

The two isolated upper teeth share characteristics of both *Lemoynea* and *Mystipterus*. *Lemoynea* is a basal desmanine talpid known from the Miocene of Nebraska (Brown 1980), which is the oldest confirmed desman in North America. The molars of *Lemoynea* are reminiscent of extant desmans: they are relatively large in size, all three upper molars have a divide mesostyle, and there are lingual cuspules on the occlusal surface of the upper molars (Brown 1980; Gunnell et al. 2008). The ETMNH teeth look very much like the teeth of *Lemoynea,* but they lack the divided mesostyle, which is a derived feature of the tribe. *Mystipterus* is a basal talpid (Uropsilinae) known from the Mio-Pliocene of Oregon. It looks more shrew-like than other talpids: there is a large hypocone flaring off the posterior aspect of the tooth, it does not have a divided mesostyle, and it does not have accessory lingual cuspules on the occlusal surface (Hutchison 1968). The ETMNH teeth have the continuous mesostyle like *Mystipterus* and other basal talpids, but lack the same generalized occlusal morphology and presence of a hypocone.

All three ETMNH teeth are distinct from the well-known fossil desman, *Archaeodesmana*. *Archaeodesmana* is known from the late Miocene – early Pliocene of Europe (Hutterer 1995). The M1 is morphologically similar to the extant species *Galemys pyrenaicus*,

with a poorly developed metastyle and a divided mesostyle. On all three lower molars, the anterolabial cingulum is well developed and sometimes there is a small cuspule on the cingulum in the re-entrant valley (Martín-Suárez et al. 2001). These characteristics are not present on any of the GFS specimens, thus cannot be called *Archaeodesmana*.

The size and morphology of these teeth are unique among fossil talpids. The size of these teeth is comparable to that of extant desmans, but larger than most fossil forms (Table 3). Though reminiscent of desmans, ETMNH 20747 and ETMNH 20779 do not possess all of the synapomorphies that have been used to define the tribe; however, all of the lower molar synapomorphies are present in ETMNH 6994. It is likely that all three teeth represent a new occurrence of stem desman, outside crown group desmans. These teeth are referred to the same taxon because the teeth are able to occlude. The second shear facet on the posterior aspect of the M1s line up with the second shear facet on the m2 (Figure 5).

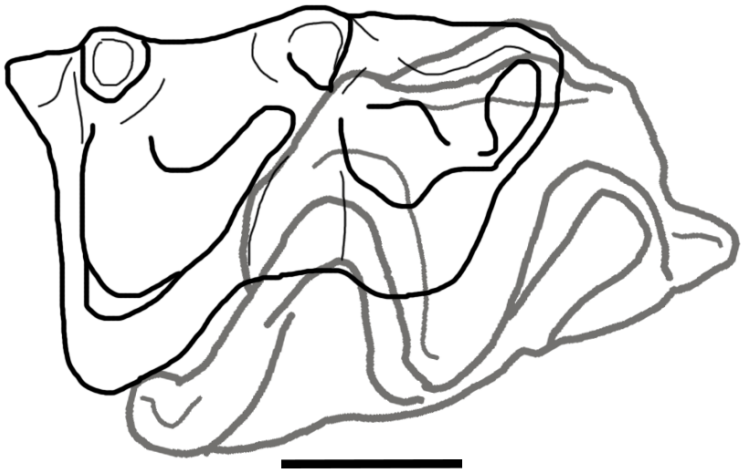

Figure 5: M1 (ETMNH 20779) superpositioned on top of m2 (ETMNH 6994). Scale bar = 1 mm.

Tribe SCALOPINI Trouessart, 1897

Genus *PARASCALOPS* True, 1894

PARASCALOPS nov. sp.

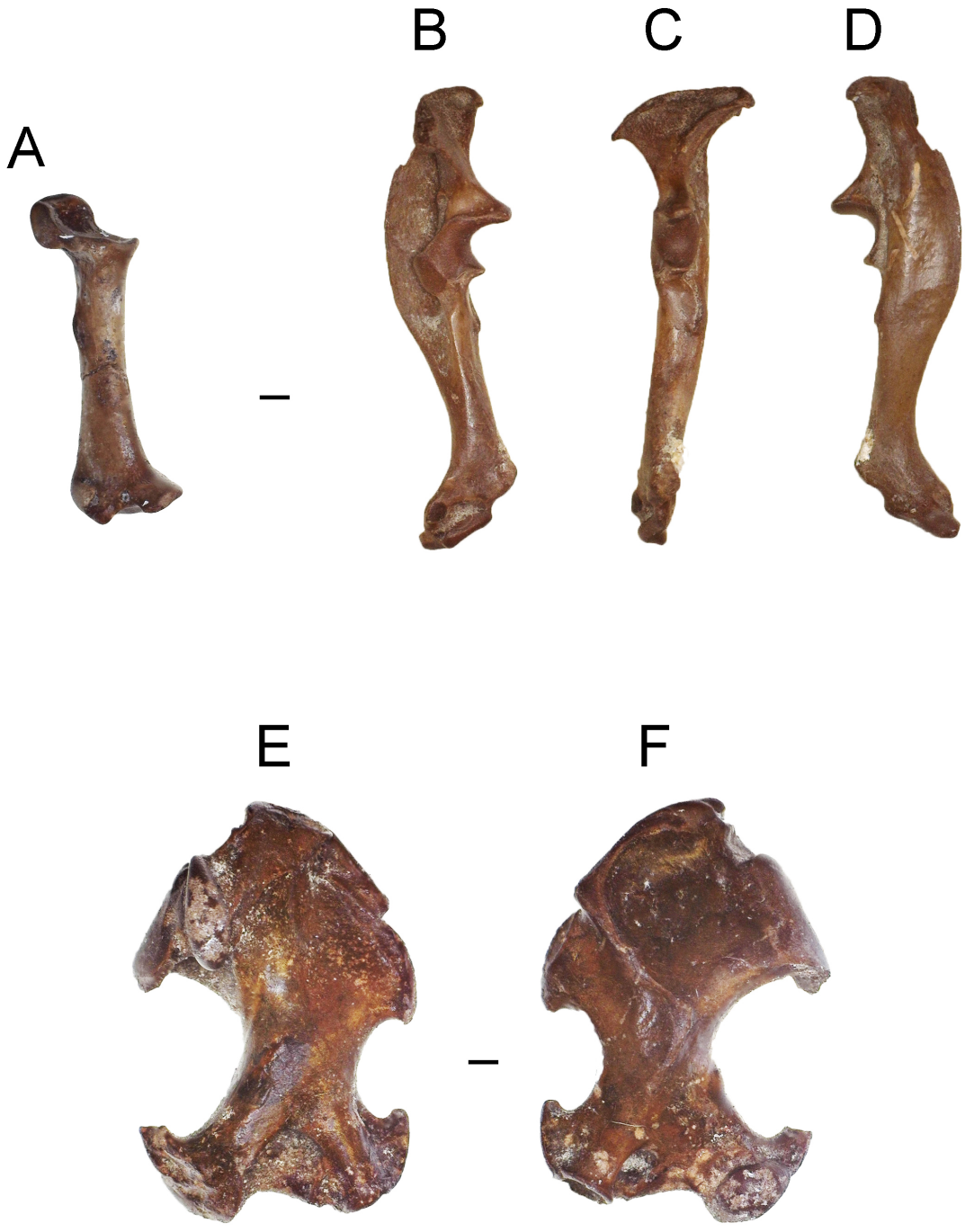

Figure 6: *Parascalops* nov. sp. material. ETMNH 14849, right radius – A) medial view. ETMNH 20748, right ulna – B) medial, C) anterior, and D) lateral views. ETMNH 6939, left humerus – E) posterior and F) anterior views. Scale bars = 1 mm.

Referred specimens – ETMNH 12305 - left humerus; ETMNH 14849 - left radius; ETMNH 20739 - right ulna; ETMNH 20736 - right humerus; ETMNH 6940 - right humerus; ETMNH 6939 - left humerus; ETMNH 20754 - right ulna, missing distal end and olecranon process; ETMNH 20748 – complete disarticulated manus (8 carpals, 5 metacarpals, 9 proximal and medial phalanges, and 5 terminal phalanges).

Locality – Gray Fossil Site, TN.

Diagnosis – Entepicondylar foramen small and laterally positioned; pectoral tubercle is a large ridge, centrally positioned and almost half of entire diaphysis length; pectoral tubercle robust; capitulum smaller and angled 20-30 degrees superiorly; ulna and radius large and robust.

Description –The humerus is longer than broad. The greater tuberosity is large and pronounced. There is a thin separation between the greater tuberosity and the humeral head. The brachialis fossa is triangular in shape. The teres tubercle is relatively large and curved proximally. There is a large gap between the entepicondylar process and the teres tubercle. The capitulum is parallel with the trochlea. The trochlea touches the fossa of the *M. flexor digitorum* ligament. The pectoral tubercle is positioned proximally and can be either a large oval tubercle (ETMNH 6940, ETMNH 12305, ETMNH 14849) or a thin ridge (ETMNH 6939, ETMNH 20736). The scalopine ridge is weakly developed, but only visible in a few specimens (ETMNH 6939 and ETMNH 20736).

In the radius (ETMNH 14849), the capitular head is broad mediolaterally with a flat, square edge. The lunar articular facet is quite large, has a curved edge, and somewhat deep. The *M. abductor pollicis* tendon groove is at a sharp angle. The distal end is large and flares

mediolaterally. There is a clean break through the center of the diaphysis that was repaired. There is no evidence of healing on this break. The distal end of the radius is relatively swollen.

The ulnae are short, mostly straight, and very robust. The proximal olecranon crest forms a sharp angle with the shaft and a large blade greatly separated from the semilunar notch. The abductor fossa is enlarged. The semilunar notch is very well defined (appears as a strong semicircle). There is a large and curved medial olecranon crest. The triceps scar is large and relatively wide. The abductor scar is elongate and makes up part of the base of the lateral olecranon crest. The distal end and the olecranon process are missing from ETMNH 20739.

There is one complete manus. All elements are completely disarticulated. There are 8 carpals, 5 metacarpals, 9 proximal and medial phalanges, and 5 terminal phalanges. All manus elements are large and robust. The carpals are blocky and large. The metacarpals and phalanges are short, anteroposteriorly compressed and mediolaterally broad. The terminal phalanges are elongate, broad, and bifurcated by large nutrient foramina.

Discussion – Osteological characters that distinguish *Parascalops* (Hairy-tailed mole) from all other known talpids include: the trochlea touches the fossa of the *M. flexor digitorum* ligament (Skoczeń 1993), the brachialis fossa has a triangular shape (Hutchison 1968), the fissure separating the greater tuberosity from the head is thin and subtle, the teres tubercle is about 1/3 the size of the pectoral ridge and has a strong curve, the scalopine ridge is weak and fragmentary with a prominence at about half of its length (Skoczeń 1993), the position of the pectoral tubercle is proximal, the groove for the tendon of *M. abductor pollicis longus* on the radius is angled sharply, the top of the capitular process of the radius is square-shaped and flat, the medial olecranon crest of the ulna is more medial and has a strong medial curve, and the brachialis scar

on the ulna is straight and thin. These characters are present on the GFS material, but morphology and size (Table 4) differences distinguish it from the extant species *Parascalops breweri*.

Table 4: Postcranial Measurements for *Parascalops*. Measurements in mm. * indicates measurement on incomplete specimens.

Taxon	Humerus length	Ulna length	Radius length
Parascalops breweri	12.3 - 15.4 (n = 22)	12.73 - 13.45 (n = 12)	8.67 - 10.11 (n = 11)
Parascalops fossilis	10.7 (n = 2)	--	--
Parascalops nov. sp.	13.48 - 15.52 (n = 4)	13.33* - 14.34 (n = 2)	10.26 (n = 1)

There are two described species within the genus *Parascalops*: *P. breweri* (extant) and *P. fossilis*. They are very similar in morphology, but have some important differences. The characters differentiating *P. fossilis* from *P. breweri* are: 1) a significantly smaller humerus, 2) shallower fossa brachialis, 3) more oblique lesser tuberosity that passes the edge of the pectoral crest to a low degree the head axis runs outside the border of the humeral shaft, and 4) the medial vascular foramen on the diaphysis is larger (Skoczeń 1993). The GFS material does not exhibit any of these morphological features.

Parascalops nov. sp. is similar in size (Table 4) and general morphology to *P. breweri*, but there are a few distinct differences. Evaluating the humerus of *Parascalops* nov. sp., the entepicondylar foramen is smaller and more laterally positioned on the diaphysis, the pectoral tubercle is a large, robust ridge, centrally positioned and almost half of entire diaphysis length, and the capitulum is smaller and angled 20-30 degrees superiorly from the ectepicondylar

process. *Parascalops breweri* humeri typically have a large entepicondylar foramen that is more medially positioned, the pectoral tubercle is a prominent lump on the diaphysis, not a ridge, and the capitulum is relatively large and angled parallel to the ectepicondylar process. The ulnae and radii of *P.* nov. sp. are more robust and physically larger (Table 4). Muscle scars on these elements are more pronounced and have more rugose texture. The distal ends of these elements also appear more swollen than those of *P. breweri*.

Parascalops nov. sp. can be differentiated from *Parascalops fossils* by size (Table 4) and general morphology. The humerus of *Parascalops* nov. sp. is large, the fossa brachialis is deep, the greater tuberosity is longer and more robust, the pectoral tubercle is large, robust and forms a ridge, and the entepicondylar foramen is small and laterally positioned. *Parascalops fossilis* has a shallow fossa brachialis, a smaller, less robust greater tuberosity, a small (almost non-existent) pectoral tubercle, and a relatively large, medially positioned entepicondylar foramen.

Parascalops nov. sp. is morphologically similar to, and falls within in the biogeographic range of, extant *P. breweri*. This taxon may be ancestral to the extant species. These fossils represent the first pre-Pleistocene record of the genus in North America and earliest record globally. This extends the known fossil history for the genus by 4 million years in North America.

Tribe CONDYLURINI Dobson, 1883

Genus *MIOSCALOPS* Ostrander et al., 1986

MIOSCALOPS sp. Ostrander et al., 1986

1950 *Mioscalops* sp.; Wilson, p. 43, fig. 34-38

2000 *Wilsonius* sp.; Kretzoi and Kretzoi, p. 230?

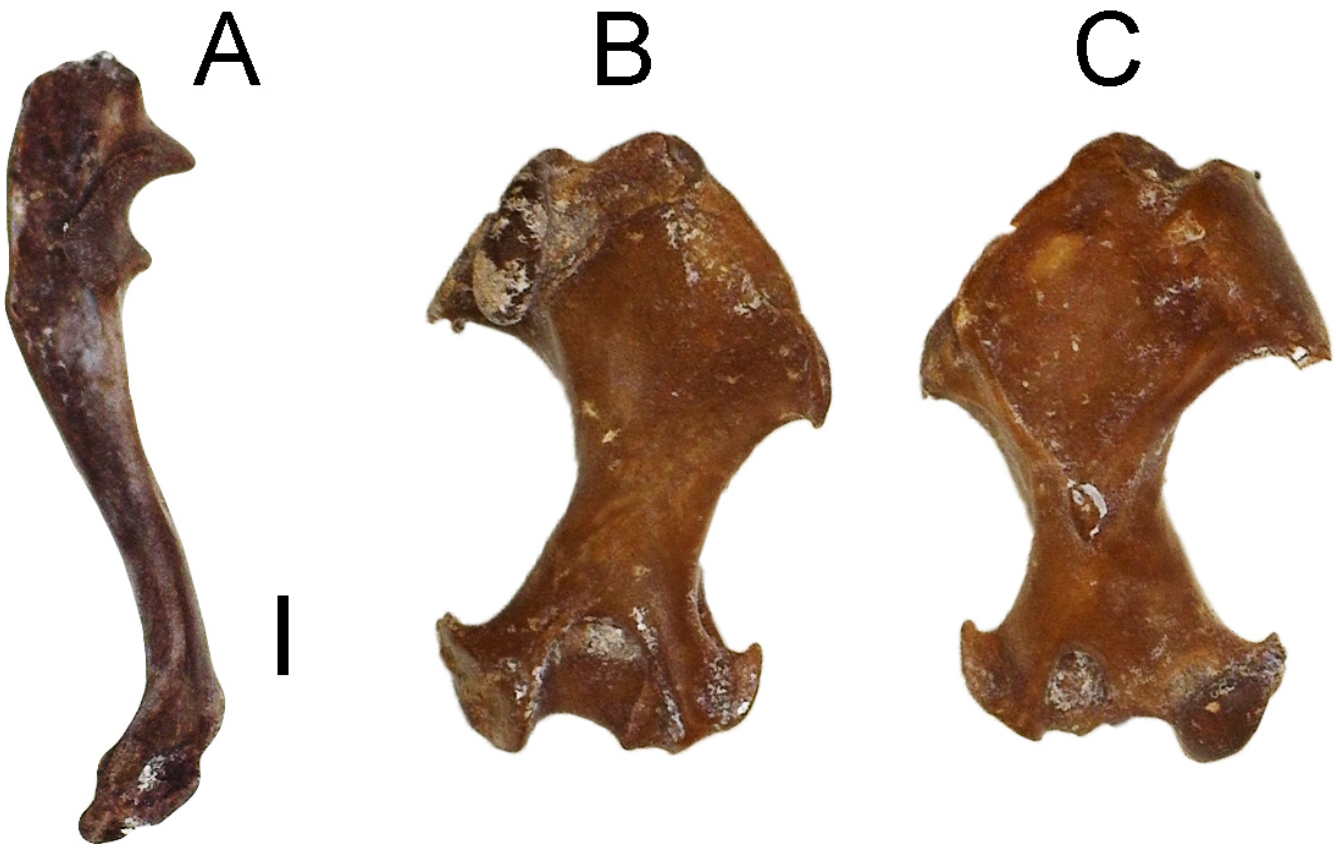

Figure 7: *Mioscalops* sp. skeletal material. ETMNH 20738, right ulna – A) medial view. ETMNH 6942, left humerus – B) posterior and C) anterior views. Scale bar = 1 mm.

Table 5: Measurements for GFS *Mioscalops* sp. * indicates measurement on incomplete specimens.

Specimen	Humerus length (mm)	Ulna length (mm)
ETMNH 6942	7.99	--
ETMNH 6943*	4.66	--
ETMNH 9565*	5.34	--
ETMNH 6941	8.02	--
ETMNH 10345*	6.16	--
ETMNH 16024	8.00	--
ETMNH 20738	--	10.12
ETMNH 20740	7.87	--
ETMNH 20743*	5.82	--
ETMNH 20744	8.03	--
ETMNH 20745*	4.59	--

Type – *Mioscalops ripafodiator*, UO 22488, right mandible with i2 and p1-m3, lacking ascending ramus, tip of the jaw anterior to the i2, and trigonid of m1. Molars heavily worn. UO loc. 2465 Quartz Basin. Age: Barstovian.

Referred specimens – ETMNH 6942 – left humerus; ETMNH 9565 – right humerus, distal end; ETMNH 6943 – left humerus, distal end; ETMNH 10345 – left humerus, distal end; ETMNH 6941 – left humerus; ETMNH 16024 – right humerus; ETMNH 20745 – right humerus, distal end; ETMNH 20740 – right humerus; ETMNH 20744 – right humerus; ETMNH 20743 – left humerus, distal end; ETMNH 20738 – right ulna.

Locality – Gray Fossil Site, TN.

Description – The humeri of this genus have a long, gracile diaphysis with ends that do not flare as mediolaterally as in extremely fossorial moles. In the anterior view, the humerus has a long shaft, with relatively narrow ends, a saddle shaped capitulum, and small entepicondylar foramen.

The position of the entepicondylar foramen is much closer to the medial aspect of the distal end. The pectoral tubercle can vary in shape from a tubercle (ETMNH 6943, ETMNH 9565, ETMNH 10345, ETMNH 20740, ETMNH 20744, ETMNH 20745) to a small ridge (ETMNH 6941, ETMNH 6942, ETMNH 20743, ETMNH 16024). The greater tuberosity is massive and not separated from the lesser tuberosity. The pectoral crest starts at the greater tuberosity and stops 2/3 of the way down the diaphysis. Most of the teres tubercle is concealed by the pectoral ridge. There are small foraminae on either side of the pectoral ridge, near the start of the pectoral tubercle.

In the posterior view of the humerus, the ectepicondylar and entepicondylar processes are angled sharply. The entepicondylar process is more robust than the ectepicondylar process. The ectepicondylar process projects laterally at a higher angle. The trochlea is mediolaterally elongated. The bicepital groove is angled medially. The teres tubercle is connected to the greater tuberosity via a thin ridge, which has a well-defined and relatively large bicepital groove. The humeral head is large when compared to other talpid taxa. The radial notch is a little depressed. The olecranon fossa is small. The capitulum is saddle shaped (convex inferiorly, concave superiorly). The entepicondylar foramen is large.

The ulna is almost complete, except that the olecranon process is broken off. The distal end flares quite a bit. This ulna is very robust despite being so small. The diaphysis is long, relatively gracile and mildly sinusoidal. There are no visible muscle scars along the diaphysis. Around the semilunar notch, the processus anconaeus greatly overhangs the notch, but the coronoid process is quite pronounced like more fossorial talpids. This trait is not common in semi-fossorial talpids.

Discussion – *Mioscalops* is the correct name to use when describing *Scalopoides* Wilson 1960. *Scalopoides* Wilson 1960, a Miocene mole, is a junior homonym of *Scalopoides* Bode 1953, a coleopteran from the Upper Lias of Europe. Therefore, the new name *Mioscalops* Ostrander et al. 1986 replaced *Scalopoides* Wilson 1960. Another genus, *Wilsonius* Kretzoi and Kretzoi 2000, was erected in Europe to describe the same Miocene talpid material; however, this genus is synonymous with *Mioscalops* Ostrander et al. 1986. Therefore, any talpid material being classified at the generic or species level as *Scalopoides* Wilson 1960 or *Wilsonius* Kretzoi and Kretzoi 2000, should be assigned to *Mioscalops* Ostrander et al. 1968.

Mioscalops has always been placed in the Scalopini tribe, but with little justification. Scalopini talpids are united by the presence of a scalopine ridge (Campbell 1939); however, this "ridge" is actually a scar that runs parallel to the greater tuberosity on the diaphysis in the posterior view of the humerus (Hutchison 1968). This character is also present in other tribes such as the Talpini, Urotrichini (Rzebik-Kowalska 2014), and Scaptonychini (Skoczeń 1980); therefore, it is not a reliable synapomorphy for the tribe Scalopini. The GFS *Mioscalops* material is morphologically similar to condylurine talpids and Gunnell et al. (2008) placed *Mioscalops* in the tribe Condylurini. Based on this evidence, *Mioscalops* is being placed here.

Mioscalops is most morphologically similar to *Scapanus*, *Condylura*, and *Scapanulus*. *Mioscalops* and *Scapanus* (Western North American moles) both have humeral heads that are in line with the diaphysis, the clavicular articular facet is semi-oval, a small teres tubercle, and a prominent scalopine ridge (Hutchison 1968); however, the genus *Scapanus* includes three species of very robust scalopine talpids and all documented fossil forms are similarly robust (Hutchison 1968; 1974; 1987). GFS *Mioscalops* is not nearly robust enough to be considered *Scapanus*.

Mioscalops also shares similarities with *Condylura* (star-nosed mole) in the proportions of the articular ends, the relative size of the teres tubercle, the shape of the humeral head, and the degree of overall robustness, but there are more differences between *Condylura* and *Mioscalops* than there are similarities. Some differences include: the direction of the humeral head, lack of scalopine ridge, clavicular articular facet being parallel to humerus long axis, strong separation from humeral head from clavicular facet, and a narrower trochlea (Hutchison 1968; 1984).

Mioscalops is morphologically similar to *Scapanulus* (Gansu mole). They have similar humeral head orientations and sizes, a scalopine ridge, a broad trochlea, an absent channel separating the humeral head from the greater tuberosity, and the proximal end of the bicepital tunnel is anteriorly visible (Hutchison 1968). The difference in teres tubercle shape and size, as well as the size of the pectoral crest differentiates *Mioscalops* from *Scapanulus*.

The name *Mioscalops* has commonly used as a "garbage-bin" taxon for any talpid found during the Miocene, but it is morphologically distinct from other Neogene talpid taxa. *Mioscalops* is known from the Oligo-Miocene through the Pliocene of North America and the Miocene of Europe (Gunnell et al. 2008). *Mioscalops* was widely distributed across North America (Figure 8) making it the most common talpid to find in a Cenozoic fossil locality that contains talpids. The *Mioscalops* material from the Gray Fossil Site is the first occurrence of a Condylurini talpid in the southeastern United States.

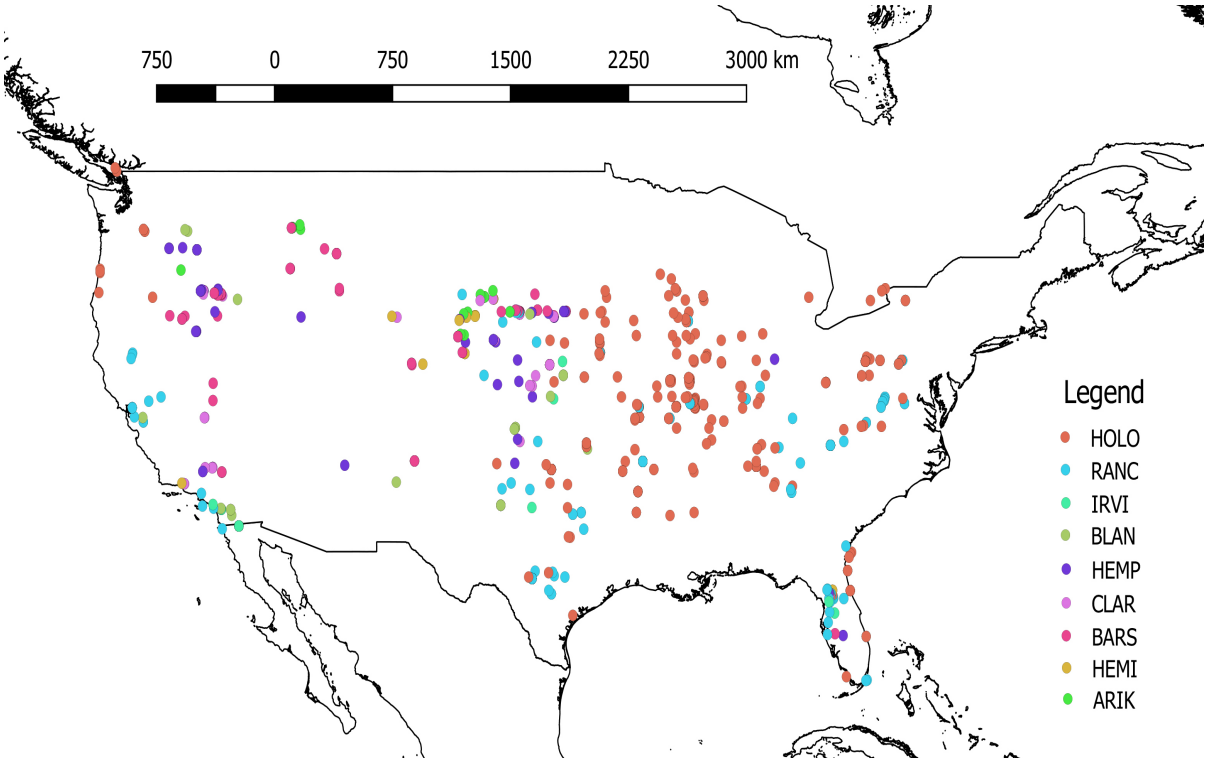

Figure 8: Map showing distribution of fossil talpid taxa across the United States by time (North American Land Mammal Ages). Data from NEOTOMA. Map made in QGIS.

Tribe NEUROTRICHINI Hutterer, 2005

Genus *QUYANIA* Storch and Qui, 1983

QUYANIA cf. *Q. EUROPAEA* Rzebik-Kowalska, 2014

1980 *Scaptonyx* (?) *dolichochir* (Gaillard); Skoczeń, p. 422, pl. 5.

1994 *Scaptonyx* (?) *dolichochir* (Gaillard); Rzebik-Kowalska, p. 80, 83, 86, 89, 92.

2005 *Urotrichus* ? *dolichochir* (?) (Gaillard); Rzebik-Kowalska, p. 123, 126, 127, 128, 129.

2009 *Urotrichus* sp.; Rzebik-Kowalska, p. 16, 19, 22, 26, 52.

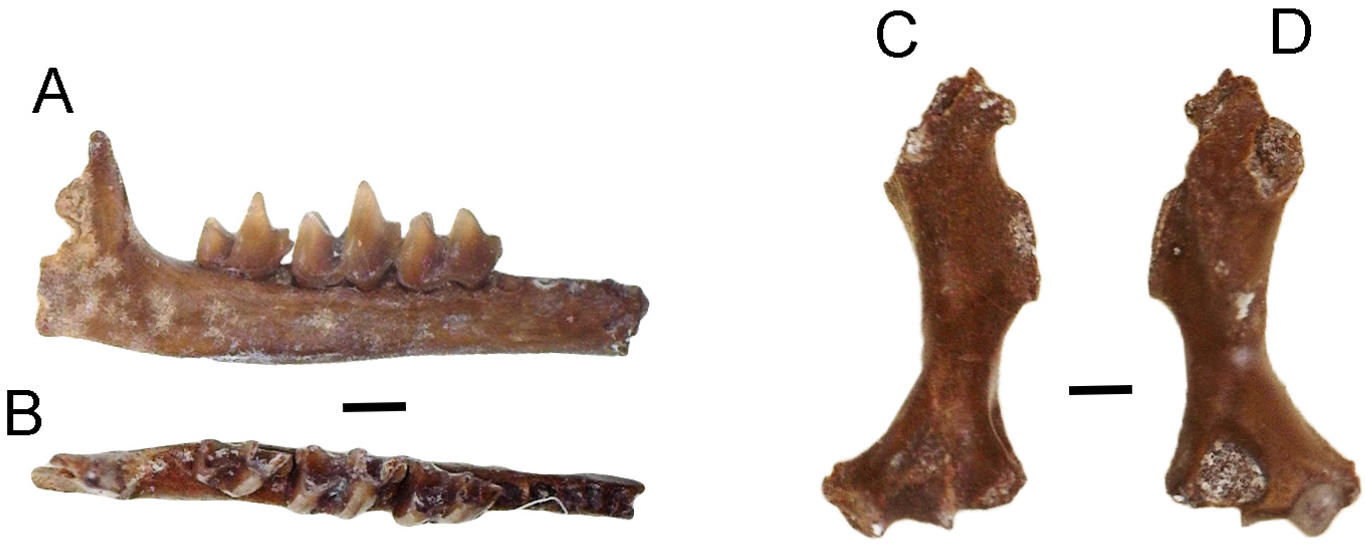

Figure 9: *Quyania* cf. *Q. europaea* skeletal material ETMNH 20737, right dentary with m1-3 – A) lingual and B) occlusal views. ETMNH 4915, left humerus – C) posterior and D) anterior views. Scale bars = 1 mm.

Table 6: Measurements for *Quyania* cf. *Q. europaea*. All measurements in mm.

Specimen	Humerus length	m1		m2		m3	
		A-P	B-L	A-P	B-L	A-P	B-L
ETMNH 4915	7.68	--	--	--	--	--	--
ETMNH 10277	5.49	--	--	--	--	--	--
ETMNH 20737	--	1.58	1.33	1.83	1.53	1.52	1.15
ETMNH 20741	--	1.50	1.29	1.82	1.48	--	--
ETMNH 16023	--	--	--	--	--	1.49	0.99
ETMNH 9728	--	--	--	--	--	1.50	1.06

Type – no. MF/1013/1, left mandibular fragment with m1 and alveoli of c-p4 and m2-m3, broken (and stuck) between p3 and p2. It is housed in the collection of the ISEAPAS in Kraków.

Rębielice Królewskie 1A, Late Pliocene, Early Villanyian, MN16.

Referred specimens – ETMNH 10277 – left humerus, missing proximal end; ETMNH 4915 – left humerus, missing proximal end; ETMNH 20737 – right dentary with m1-3; ETMNH 16023 – right m3; ETMNH 9713 – left edentulous dentary; ETMNH 9728 – left m3 with posterior dentary fragment; ETMNH 20741 – left dentary with m1-2.

Locality – Gray Fossil Site, TN.

Description – The humerus is quite gracile; it is long and thin with minimal flaring projections on the distal end. The pectoral ridge narrows to a point about half way down the diaphysis. ETMNH 10277 has less of pectoral ridge present on the diaphysis than ETMNH 4915. The teres tubercle is long, relatively robust, and rather rectangular. In the anterior view, the olecranon fossa has a distinct concave notch at the base towards the center. The olecranon fossa is horseshoe shaped and asymmetrically slanted medially. In the posterior view, the trochlea is relatively dorsoventrally elongated and narrowed mediolaterally. There is a groove in between the trochlea and the entepicondylar process along the distal-most aspect of the humerus. This gives the distal end of the humerus an asymmetrical appearance. The medial epicondyle is really chunky and probably had a large process on it. The entepicondylar foramen is visible just above the medial epicondyle and is quite large. The entepicondylar foramen is very large.
The entepicondylar process is a small projection sticking off the medial aspect. The capitulum is very small and oval-shaped.

The dentary is thin and gracile. There is minimal curving along the inferior margin of the dentary. The greatest point of curvature is below the talonid basin of m2 and the trigonid of m3. The anterior mental foramen is positioned under p2 (not present in ETMNH 20737 which has p3 alveolus). There is a small gap between m3 and the ascending ramus.

In the m1, the talonid is buccolingually elongated, but it is about the same size as the trigonid. The talonid is about the same height as the trigonid. The cristid obliqua terminates anteriorly (buccally) and is separated by a small notch from the posterior wall of the trigonid. The protoconid is the tallest cusp, and then metaconid, with the paraconid as the shortest cusp. The metaconid and paraconid have wear on their buccal aspect. The paraconid has a bladed notch along the posterior aspect. The entoconid and hypoconid are distinct. There is a small posterior accessory cusp on the posterior aspect of the entoconid. There is a strong hypoflexid between the hypoconid and protoconid. There is a well-formed entocristid between the entoconid and the metaconid. The postfossid is relatively deep, but not as deep as in the m2.

In the m2, the trigonid is taller than the talonid. The trigonid is smaller anterioposteriorly than the talonid. The talonid has a strong hypoconid and entoconid. The protoconid is the tallest cusp, then metaconid, and the paraconid is the shortest cusp. The paraconid has a bladed notch along the posterior aspect. There is a tiny posterior accessory cuspid just posterior to the entoconid. There is a strong hypoflexid between the hypoconid and protoconid. The postfossid is very deep. An entocristid is present, but weak.

The m3 is longer anterioposteriorly than buccolingually. The trigonid flares anterioposteriorly (paraconid and metaconid diverge from one another) making it appear very open. The talonid is also very open. The talonid is lower than trigonid, but the trigonid is smaller. The paraconid has a bladed notch along the posterior aspect. There is a distinct hypoconid, and evidence for an entoconid in some specimens (not present in ETMNH 20737, but present in ETMNH 16023 and ETMNH 9728). The entoconid is large and has a well-formed posterior accessory cuspid present. There is no hypoconulid.

Discussion – There has been a debate about the hierarchical classification of the genus *Quyania*. Storch and Qui (1983), place the genus in the Urotrichini based on the morphological similarities to the extant species *Urotrichus talpoides* (Japanese shrew mole), but a recent morphological analysis by Rzebik-Kowalska (2014) showed that ?*Neurotrichus polonicus* from Poland has characters of both extant *Neurotrichus* and *Quyania*. The teeth and humeri of *N. polonicus* are similar in size to extant *Neurotrichus*, but larger than *Quyania*. The first mental foramen in the mandible is either positioned before p3 like *Quyania* or below the first root of p3 like extant *Neurotrichus*. Lower molars from geologically older specimens have vestigial mesoconids and small notches between the end of crista obliqua and the posterior wall of the trigonid like *Quyania*, but geologically younger teeth have lower molars lacking mesoconids and notches like extant *Neurotrichus*. Currently, He et al. (2016) has Urotrichini and Neurotrichini hypothesized as sister tribes, so it is unsurprising that researchers have had difficulty placing this extinct genus in one tribe or the other. Based on the more recent morphological evidence from Rzebik-Kowalska (2014), *Quyania europaea* is being placed in the Neurotrichini here.

The teeth of shrew moles tend to be low crowned and the upper molars have a small accessory cuspule (Skoczeń 1980) that resembles/functions like a hypocone. The lower molars usually have a posterior accessory cuspule, like Desmanini talpids. The size of the accessory cuspule varies depending on the tooth and taxon, but it is quite large in the tribe Urotrichini. All shrew moles have a distinct bladed crest along the posterior aspect of the paraconid in all three lower molars.

The genus *Quyania* is defined by having the crista obliqua of the m1: 1) terminate anteriorly (buccally) and 2) separated by a small notch from the posterior wall of the trigonid (Storch and Qui 1983; Rzebik-Kowalska 2014). *Quyania* is differentiated from *Neurotrichus* by

the presence of a mesoconid on m1, the cristid obliqua being separated from the posterior wall of the trigonid by a clear notch on the m1, and the first mental foramen being present under p2 (Rzebik-Kowalska 2014). In *Neurotrichus*, the m1 does not have a mesoconid, the cristid obliqua is not separated from the trigonid by a notch, and the first mental foramen is under p3.

Quyania europaea is differentiated from *Quyania chowi* by a more slender shaft of the humerus, more delicate "scalopine ridge", a narrower precingulid in m1, and the talonids of m1 and m2 closed by a well-developed ridge connecting the metaconid with the entoconid (Storch and Qui 1983; Rzebik-Kowalska 2014). *Quyania europaea* is differentiated from *Quyania* aff. *polonica* by the presence of a mesoconid (Rzebik-Kowalska 2014).

The humeral morphology of *Quyania europaea* resembles that of *Quyania chowi*, *Neurotrichus gibbsii* (American shrew mole), *Urotrichus talpoides* (Japanese shrew mole), and *Dymecodon pilirostris* (True's shrew mole). All of these taxa have similar general morphology: a long, gracile humeral diaphysis with enlarged teres tubercle, reduced greater tuberosity, reduced lesser tuberosity that also projects medially, and deep bicepital groove; however, all species in *Quyania* have a small notch between the pectoral ridge and the teres tubercle (Storch and Qui 1983), while the extant species do not have this feature. The humerus of *Q. europaea* can be differentiated from that of *Q. chowi* based on a more slender shaft and a more delicate "scalopine ridge" (Rzebik-Kowalska 2014). The humerus of *Q. europaea* can be differentiated from all extant species based on a more slender humeral shaft, smaller greater tuberosity, weaker pectoral tubercle, and more space between the distal end of the greater tuberosity and the proximal end of the teres tubercle.

Quyania europaea is only known from the Plio/Pleistocene of Poland, making the GFS specimens the first occurrences of this taxon outside of Europe.

CHAPTER 4

RESULTS

Relative Warps Analysis

Relative warp analysis yielded 3 relative warp axes that account for 88.26% of variance in humerus shape (Figure 10). Relative warp 1 (RW1) accounts for 78.75% of total variation in humerus shape. RW1 shows a reduced greater tuberosity, an elongated lesser tuberosity, a proximodistally reduced, mediolaterally elongated teres tubercle, and greater mediolateral elongation of the distal end in the positive direction. The diaphysis is greatly mediolaterally compressed and both the lesser and greater sulci are enlarged in the positive direction. The negative direction shows an enlarged greater tuberosity, reduced lesser tuberosity, a proximodistally elongated, mediolaterally reduced teres tubercle, and mediolateral compression of the distal end. The head of the capitulum is reduced in size and oriented more laterally in the negative direction. There is also greater reduction of the trochlea in the negative direction.

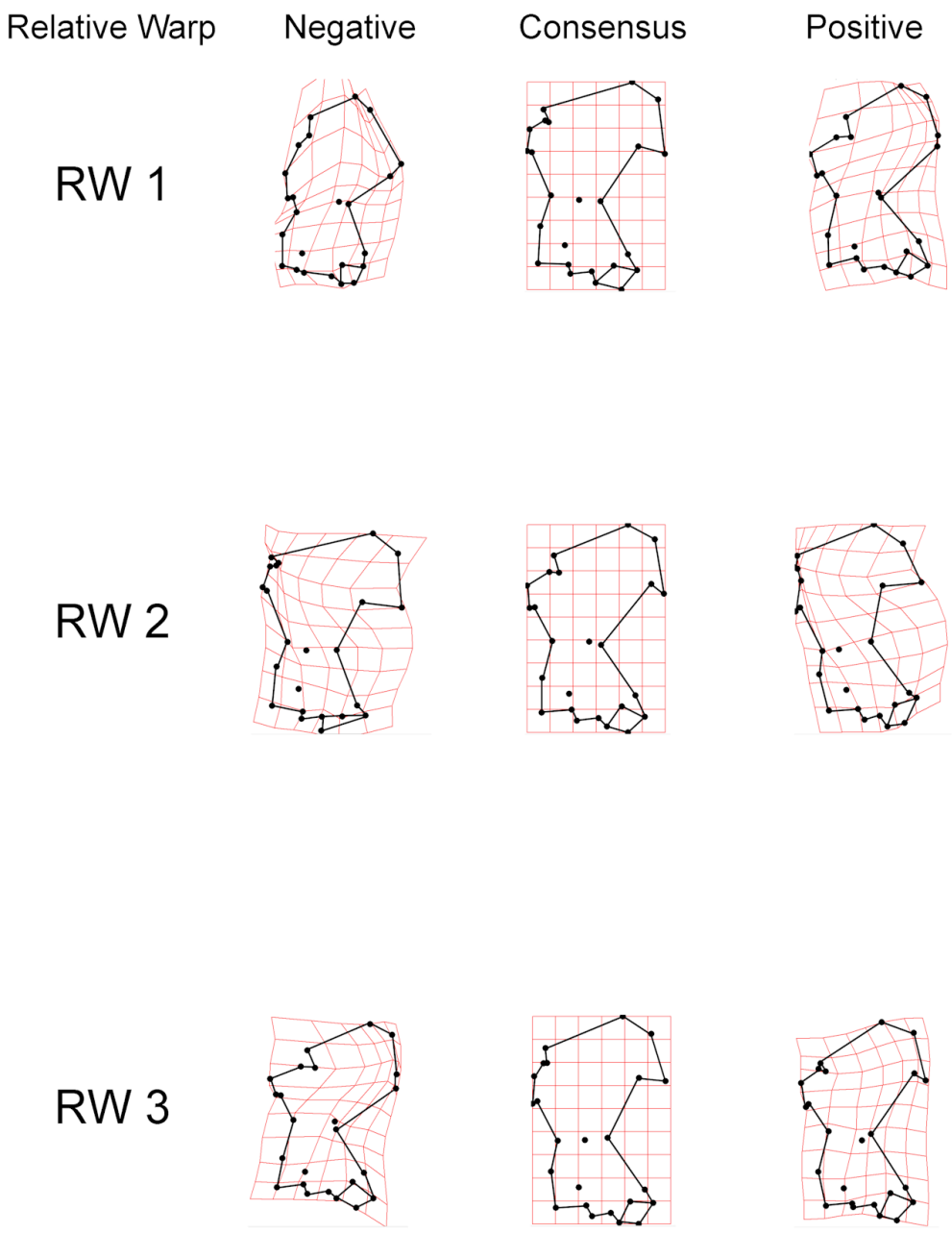

Figure 10: Relative warps analysis thin plate splines showing grid deformation in positive and negative directions to achieve change in humerus shape per relative warp. The consensus shape per relative warp is shown in the center.

Relative warp 2 (RW2) accounts for 6.28% of total variance. RW2 shows a reduction of the greater and lesser tuberosities, an elongation of the teres tubercle, and an enlarged trochlea and capitulum in the positive direction. Both the proximal and distal ends are mediolaterally compressed in the positive direction. The entire humerus is oriented more laterally, where the deltoid process is in line with the medial-most aspect of the capitulum. In the negative direction, there is elongation of both the greater and lesser tuberosities, a reduction in the teres tubercle, and greatly reduced trochlea and capitulum. Both the proximal and distal ends are mediolaterally elongated, but the diaphysis is proximodistally compressed.

Relative warp 3 (RW3) accounts for 3.23% of total variance. RW3 shows a proximodistally reduced teres tubercle, a reducted trochlea, and enlarged and laterally oriented capitulum, and a well developed deltoid process in the positive direction. The medial-most edge of the greater tuberosity does not overhang the medial-most edge of the capitulum. In the negative direction, there is a slightly reduced lesser tuberosity, a greatly mediolaterally elongated teres tubercle, a more laterally positioned trochlea, a reduced capitulum that is more medially oriented, and a very reduced deltoid process. The diaphysis is greatly mediolaterally compressed in the negative direction.

Canonical Variate Analysis

The canonical variate analysis using partial warp scores as variables yielded 3 canonical variates, which explained 100% of the variance in humerus shape and found significant separation of locomotor groups (Wilks' $\lambda = 0.001$, $P < 0.001$) (Table 7); Canonical Variate 1 (CV1) accounts for 75% of the variance and separates fossorial taxa from non-fossorial ones (Figures 11 and 12). CV1 separates fossorial talpids, with humeral diaphysis compression and articular end elongation, at the positive end from non-fossorial talpids, with humeral diaphysis

elongation and articular end compression, at the negative end. The teres tubercle is proximodistally compressed, the deltoid process is sharp and angled distally, the pectoral tubercle is more medially positioned and more distally placed on the diaphysis, the fossa for the *M. flexor digitorum* ligament is more distal at the positive end compared to teres tubercle elongation, weakly angled deltoid process, more centrally and laterally placed pectoral tubercle, and the entepicondylar foramen is more proximal at the negative end.

Table 7: Eigenvalues, % Variance of Axes, and Wilks' Lambda

Function	Eigenvalue	% of Variance	Canonical Correlation	Wilks' Lambda	Significance
CV1	35.635	75.0	0.986	0.001	0.000
CV2	10.244	21.6	0.954	0.034	0.000
CV3	1.362	3.4	0.787	0.380	0.000

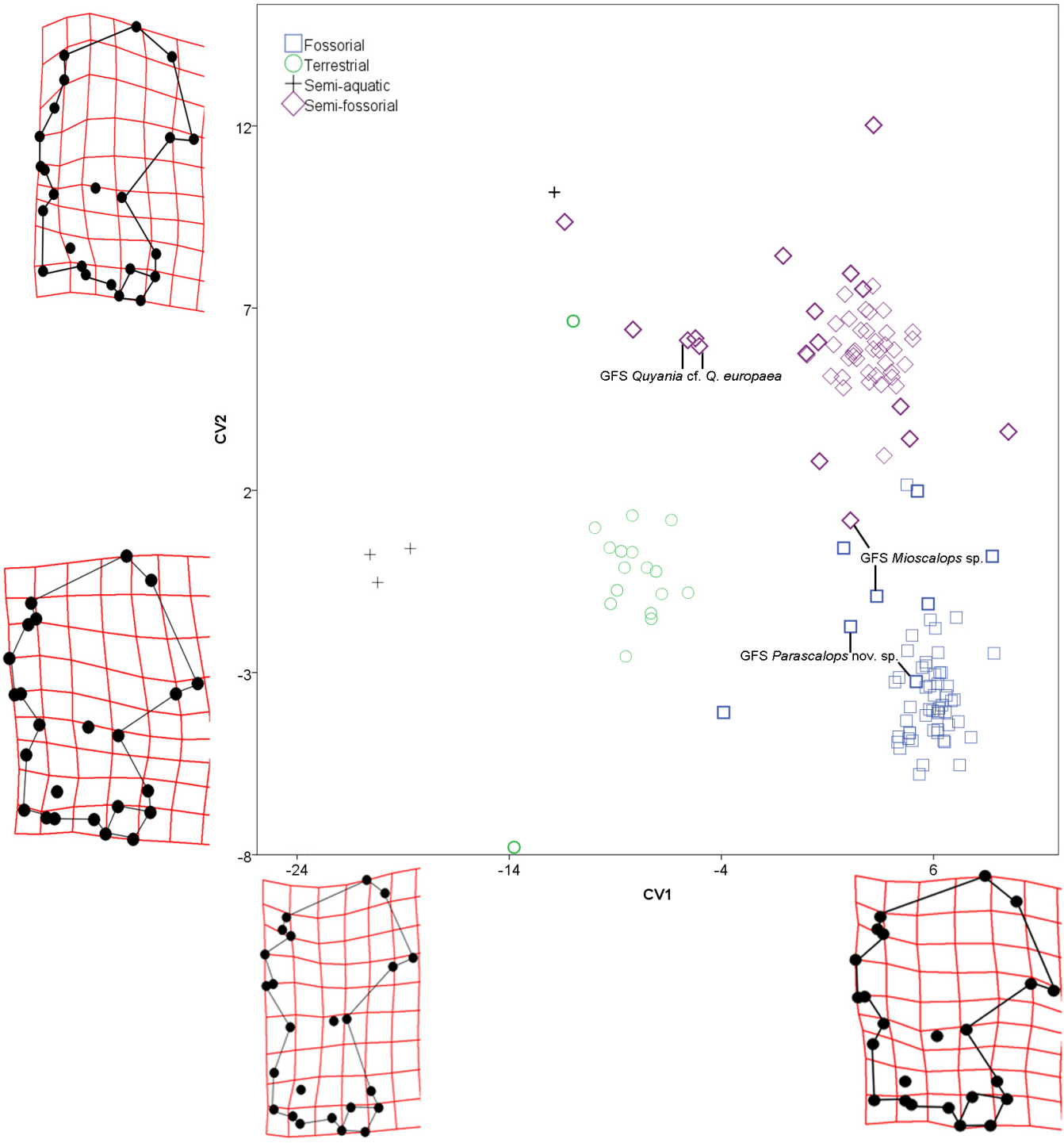

Figure 11: Plot of humerus shape based on canonical variates one (CV1) and two (CV2). Deformation grids show change in shape along each axis in positive and negative directions. Fossils taxa are bold. GFS taxa are labeled.

Canonical Variate 2 (CV2) has the second highest variance at 21.6% and separates fossorial taxa from semi-fossorial taxa (Figure 12). CV2 separates semi-fossorial forms, with more mediolateral compression of the proximal end, a larger bicepital groove, more distally positioned teres tubercle, and mediolateral elongation of the distal end, at the positive end from fossorial specialists, with mediolaterally flaring proximal end, elongated greater tuberosity, reduced bicepital groove, proximally positioned teres tubercle, and mediolateral compression of the distal end, at the negative end. On the positive end, the entepicondylar foramen is positioned more laterally to the trochlea, whereas the entepicondylar foramen is in line with the lateral margin of the trochlea at the negative end.

Canonical Variate 3 (CV3) accounts for only 3.4% of variance and separates terrestrial taxa from semi-aquatic taxa (Figure 13). CV3 separates semi-aquatic forms, with diaphysis proximodistal elongation, major reduction of the proximal and distal ends, reduced teres tubercle, and reduced capitulum, at the positive end from more terrestrial forms, with less proximodistal elongation, mediolateral flaring of proximal and distal ends, and well-developed teres tubercle and capitulum, at the negative end.

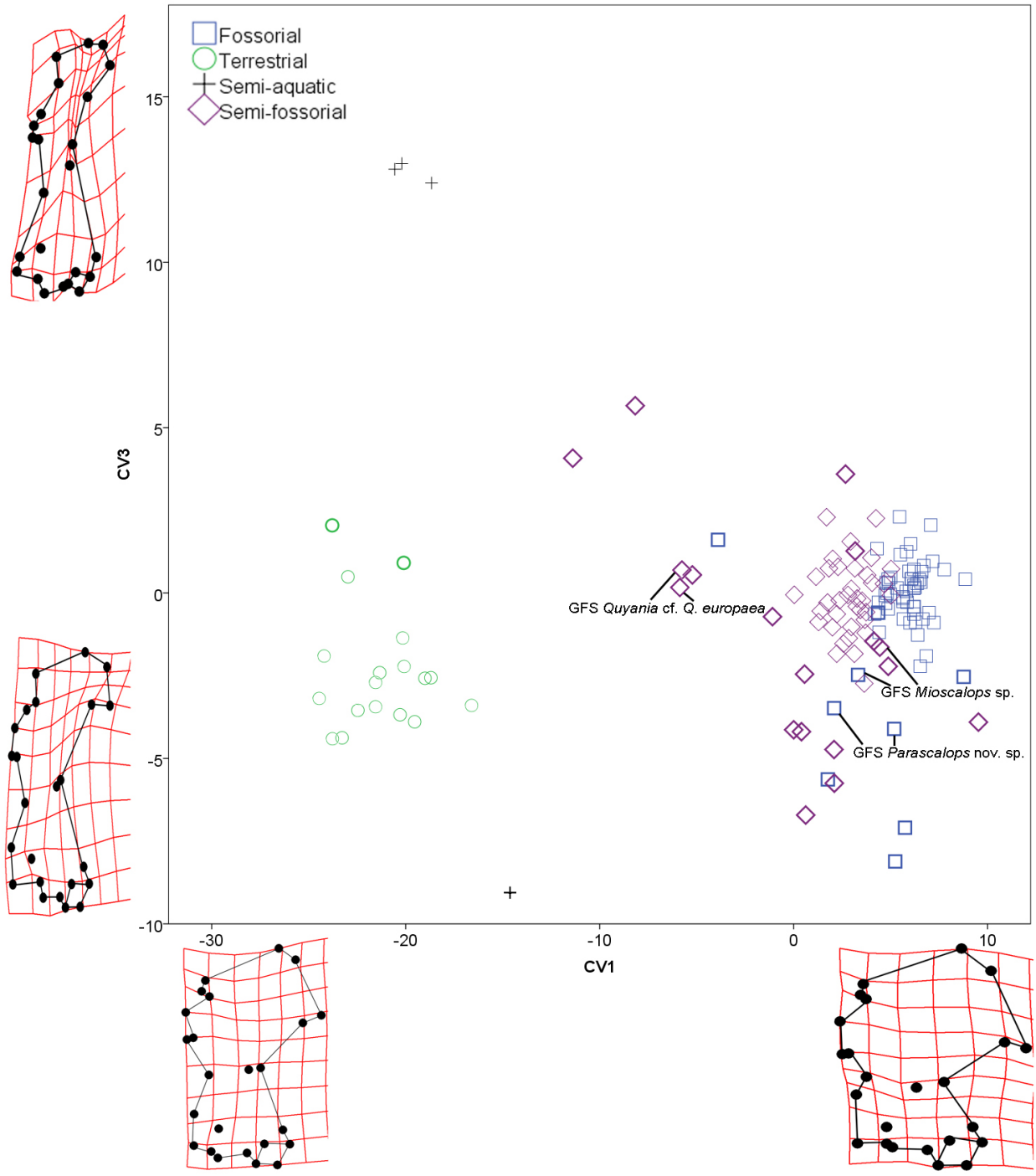

Figure 12: Plot of humerus shape based on canonical variates one (CV1) and three (CV3). Deformation grids show change in shape along each axis in positive and negative directions. Fossils taxa are bold. GFS taxa are labeled.

The analysis correctly classified locomotor groups in 99.2% of original grouped cases and 95.5% when cross-validated (Table 8). Over half (n=17) of the fossil taxa were classified as semi-fossorial (Table 9), but a few classified as semi-aquatic (n = 1) and terrestrial (n = 2). GFS *Quyania* cf. *Q. europaea* specimens were classified as semi-fossorial. GFS *Mioscalops* sp. specimens were classified as both semi-fossorial and fossorial, while GFS *Parascalops* nov. sp. specimens were classified as fossorial.

Classifications of fossil taxa resulted in high posterior probabilities and low conditional probabilities (Tables 9). This indicates that fossil taxa are close to the centroid for a particular group (high posterior probability), but outside of the observed clustering for that group (low conditional probability), as indicated by their intermediate positions in morphospace (Figure 13).

Table 8: Canonical Variates Analysis Classification for All Talpids

			Predicted Group Membership				Total
		Category	Fossorial	Terrestrial	Semi-aquatic	Semi-fossorial	
Original	Count	Fossorial	57	0	0	0	57
		Terrestrial	0	18	0	0	18
		Semi-aquatic	0	0	4	0	4
		Semi-fossorial	1	0	0	53	54
	%	Fossorial	100.0	0.0	0.0	0.0	100.0
		Terrestrial	0.0	100.0	0.0	0.0	100.0
		Semi-aquatic	0.0	0.0	100.0	0.0	100.0
		Semi-fossorial	1.9	0.0	0.0	98.1	100.0
Cross-validated	Count	Fossorial	57	0	0	0	57
		Terrestrial	0	16	2	0	18
		Semi-aquatic	0	0	3	1	4
		Semi-fossorial	2	0	1	51	54
	%	Fossorial	100.0	0.0	0.0	0.0	100.0
		Terrestrial	0.0	88.9	11.1	0.0	100.0
		Semi-aquatic	0.0	0.0	75.0	25.0	100.0
		Semi-fossorial	3.7	0.0	1.9	94.4	100.0

Table 9: Classification of Fossils. P(D/G) represents the conditional probability of the observed discriminant function score, given membership in the most likely group. P(G/D) represents the posterior probability that a case belongs to the predicted group, given the sample used to create the discriminant model.

Case	Taxon	Predicted group	P(D>d | G=g)	P(G=g | D=d)
88	*Condylura kowalskii*	Semi-fossorial	0.291	1.000
89	*Desmanella gudrunae*	Terrestrial	0.749	1.000
90	*Desmanodon crocheti*	Semi-fossorial	0.244	1.000
91	*Desmanodon fluegeli*	Semi-fossorial	0.921	1.000
92	*Gaillardia thompsoni*	Terrestrial	0.272	1.000
96	*Geotrypus montisasini*	Semi-fossorial	0.503	1.000
97	*Leptoscaptor robustor*	Fossorial	0.440	1.000
98	*Mioscalops* sp ETMNH 6941	Semi-fossorial	0.211	1.000
99	*Mioscalops* sp. ETMNH 6942	Fossorial	0.122	1.000
100	*Mygalea magna*	Semi-aquatic	0.001	0.521
101	*Myxomygale minor*	Semi-fossorial	0.000	1.000
102	*Neurotrichus polonicus*	Semi-fossorial	0.351	1.000
103	*Parascalops* nov. sp. ETMNH 6939	Fossorial	0.009	1.000
104	*Parascalops* nov. sp. ETMNH 6940	Fossorial	0.561	1.000
105	*Parascalops fossilis*	Fossorial	0.253	1.000
106	*Proscapanus sansansiensis*	Semi-fossorial	0.327	1.000
107	*Quyania chowi*	Semi-fossorial	0.177	1.000
108	*Quyania europaea*	Semi-fossorial	0.088	1.000
109	*Quyania polonica*	Semi-fossorial	0.645	1.000
110	*Mioscalops* sp. A	Semi-fossorial	0.120	1.000
111	*Mioscalops ripafodiator*	Semi-fossorial	0.228	1.000
112	*Mioscalops* sp. E	Semi-fossorial	0.270	1.000
113	*Tenuibrachiatum storchi*	Semi-fossorial	0.635	1.000
122	*Yanshuella primaeva*	Semi-fossorial	0.003	0.977
123	*Yunoscaptor scalprum*	Semi-fossorial	0.087	1.000
134	*Quyania* cf. *Q. europaea* ETMNH 4915	Semi-fossorial	0.092	1.000
135	*Quyania* cf. *Q. europaea* ETMNH 10277	Semi-fossorial	0.080	1.000

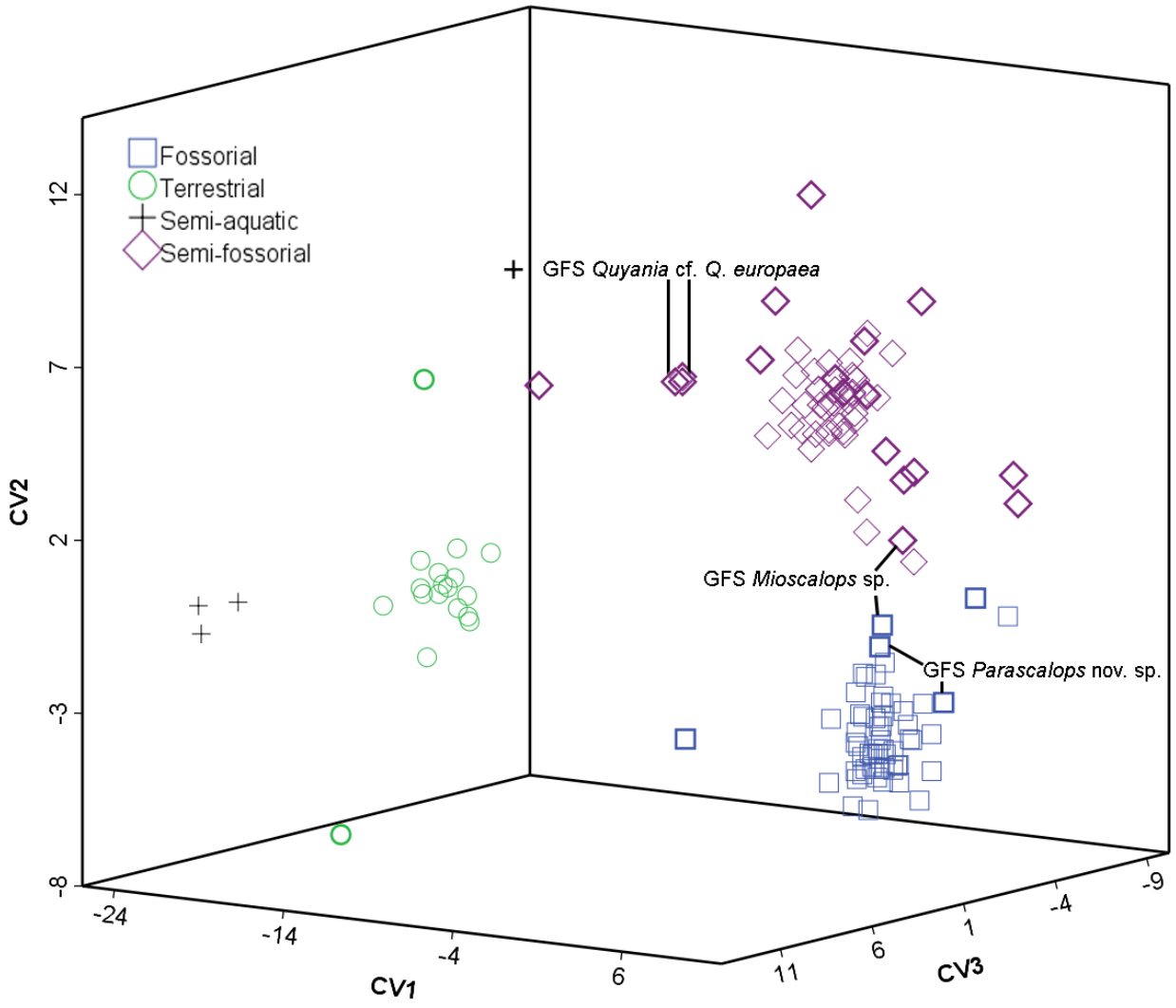

Figure 13: CVA plot shows ecological separation among the 3 main functions. Locomotor ecologies are represented by shape and color. Fossils taxa are bold. GFS taxa are labeled.

Hierarchical Cluster Analysis

Using Hierarchical Cluster Analysis, two phenograms were generated: one depicting all individuals included in the analysis and the other based on species mean values for partial warps. In the individual phenogram (Figure 14), almost all of the species within the same genus clustered together, though there were not enough variables to prevent large polytomies. There are a few genera with species that clustered into different groups, such as *Urotrichus soricipes* grouping with Soricidae and the Desmanini rather than the other shrew moles [Scaptonychini, Urotrichini, and Neurotrichini], and *Quyania europaea*† clustering with *Dymecodon pilirostris* rather than the other 2 species of *Quyania*†.

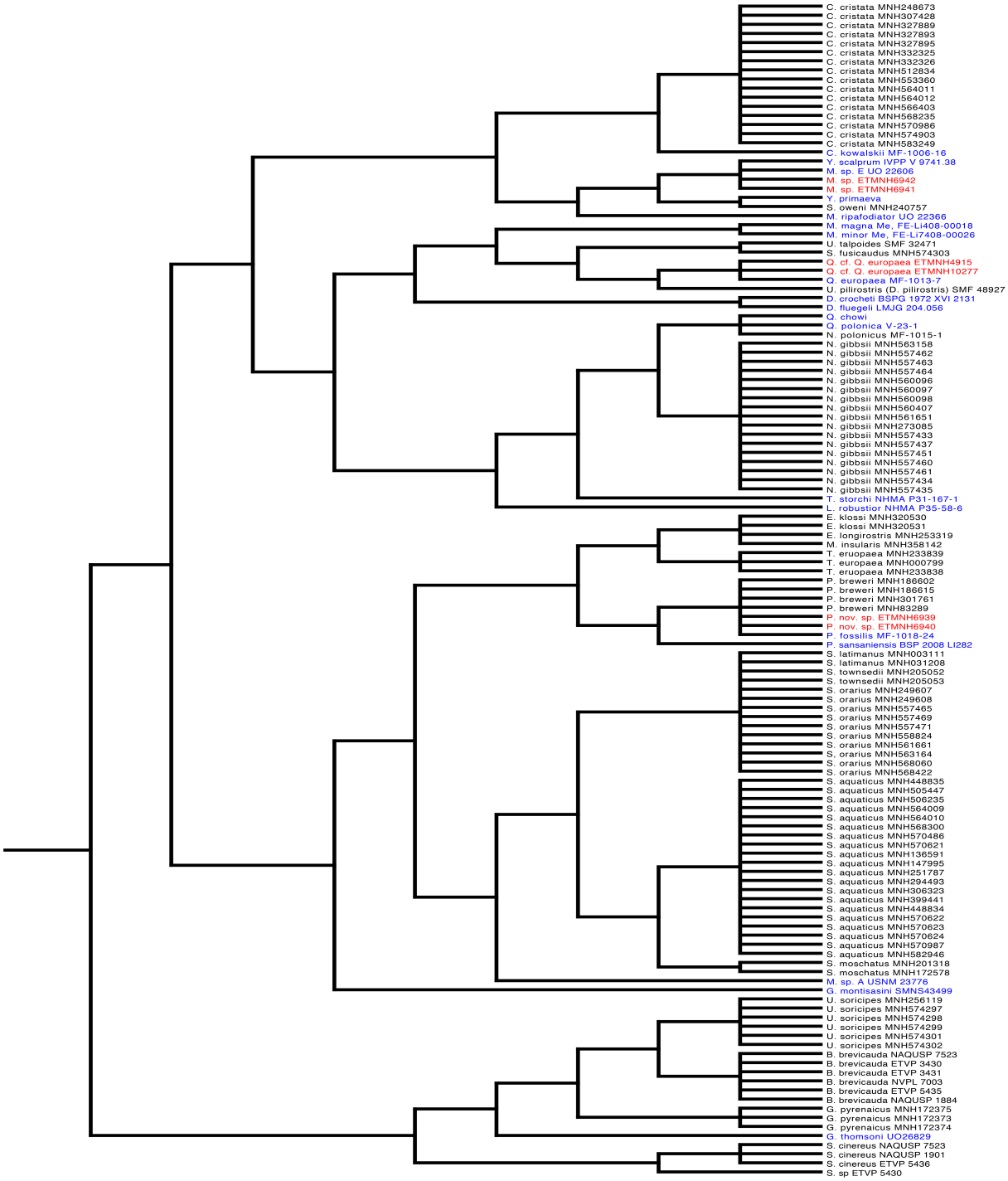

Figure 14: Individual taxon phenogram based on squared Euclidean distance. Fossil taxa are in blue. Gray Fossil Site taxa are in red.

The species mean phenogram (Figure 15) shows the average clustered position for each taxon. This phenogram has been color-coded to make comparisons with the He et al. (2016) phylogeny easier. There are six distinct clusters that resemble well-known tribes defined by He et al. (2016) (Figure 1), but their positions differ slightly. The cluster analysis suggests Condylurini and the shrew mole cluster (Scaptonychini, Neurotrichini, and Urotrichini) are similar and that *Uropsilus* is morphologically separated from Talpinae, which agrees with the He et al. (2016) molecular hypothesis. The cluster analysis grouped *Uropsilus* (Uropsilinae), *Galemys* (Desmanini), and *Gaillardia*† with Soricidae (true shrews represented by *Sorex* and *Blarina*) and grouped the Talpini and Scalopini clusters together.

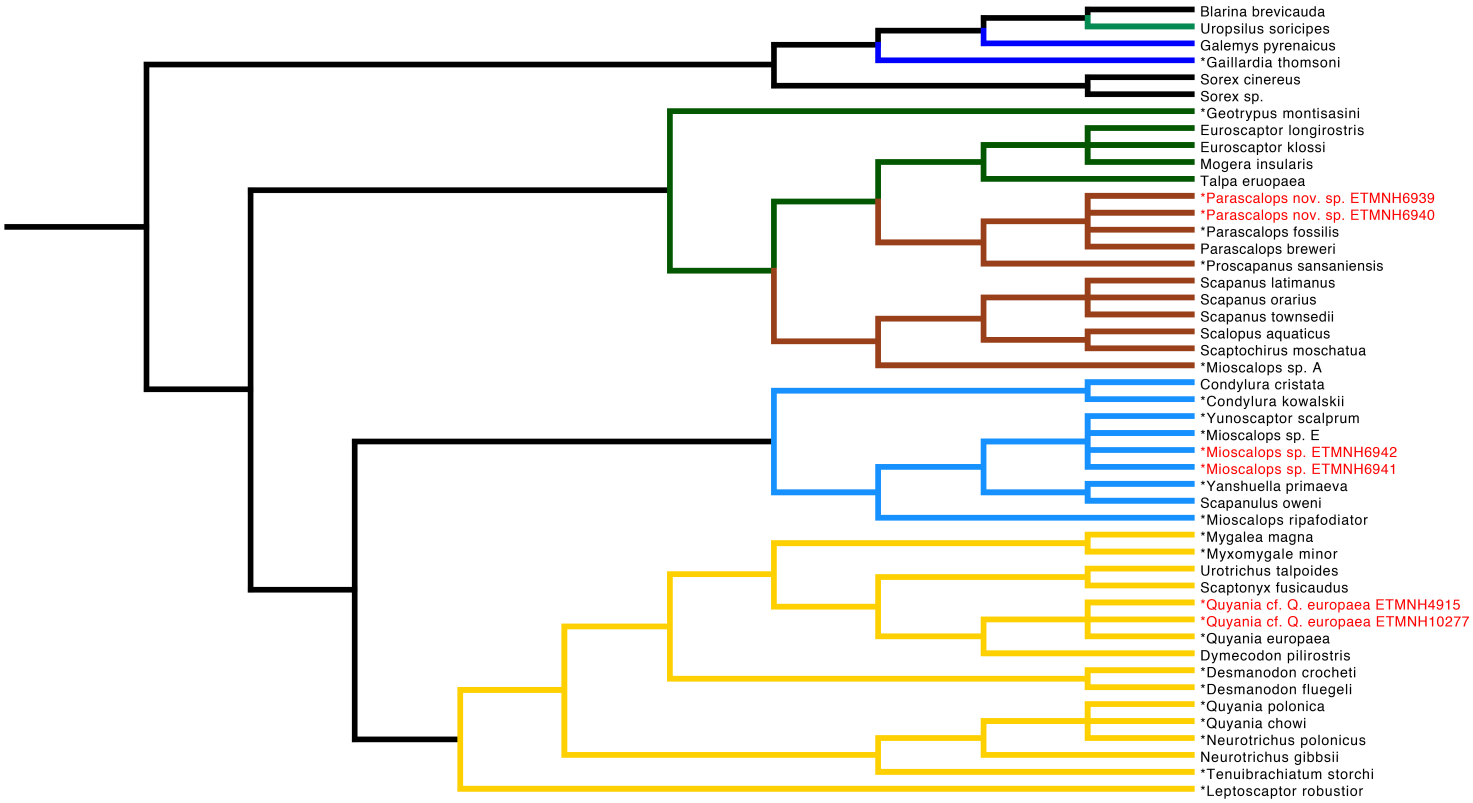

Figure 15: Average position phenogram. Major clusters color-coded to match He et al. (2016). GFS taxa in red.

The Gray Fossil Site taxa clustered with 3 separate groups: Scalopini (*Parascalops* nov. sp.), Urotrichini (*Quyania* cf. *Q. europaea*), and Condylurini (*Mioscalops* sp.). GFS *Parascalops* nov. sp. clustered with all individuals in the genus *Parascalops*, which includes extant *P. breweri* (Hairy-tailed mole) and *P. fossilis*†, along with *Proscapanus sansansiensis*†. GFS *Quyania* cf. *Q. europaea* clustered with the other *Q. europaea*† and extant *Dymecodon pilirostris* (True's shrew mole). GFS *Mioscalops* clustered with *Mioscalops* sp. E†, *Yunoscaptor scalprum*†, *Yanshuella primaeva*†, *Scapanulus oweni* (Gansu mole), *Mioscalops ripafodiator*†, *Condylura kowalskii*†, and *Condylura cristata* (Star-nosed mole).

Both phenograms created by the cluster analysis verified that that there are at least four distinct clusters, six if the two groups that clustered with the outgroup are included. The analysis clustered the Talpini and Scalopini groups together, but also shows distinct separation between the two from one another. The analysis was also able to recreate the shrew mole (Scaptonychini, Urotrichini, and Neurotrichini) and the Condylurini clusters.

Ancestral State Reconstruction

To look at changes in body size through time (Figure 16), I used humerus length as a proxy for body size and added it as a character to trace through time on the cluster analysis results. I used maximum parsimony to dictate how characters would change through time. The most common size ranges for humerus length are between 6 – 9 mm and 13 – 17 mm. Two taxa show evidence for gigantism, *Gaillardia thomsoni*† and *Scapanus townsedii* (Townsend's mole), in their respective clusters. The analysis determined that the ancestral state for humerus size for the family was between 10 and 12 mm.

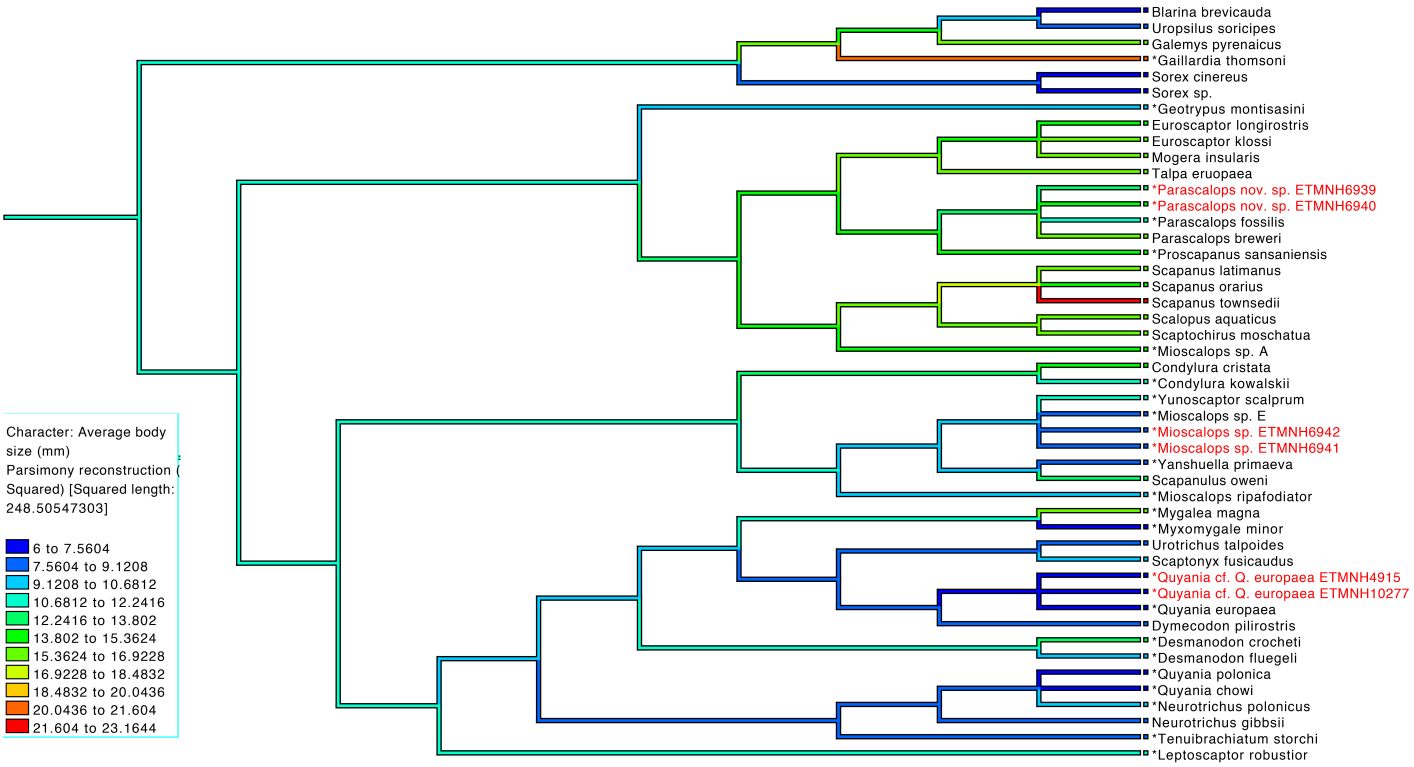

Figure 16: Ancestral state reconstruction of humerus size in mm (used as a proxy for body size). GFS taxa in red.

I also looked at the evolution of locomotor specialization through time by tracing the locomotor ecologies onto the cluster analysis results (Figure 17). The most prominent trend is the separation of the terrestrial group from the fossorial group. The terrestrial group consists of the outgroup and the few talpid taxa that could not be differentiated from the outgroup (*Uropsilus* (Chinese shrew mole), *Galemys* (Pyrenean desman), and *Gaillardia*†). *Galemys* is the only semi-aquatic talpid on the tree. All of the other lineages have some combination of fossorial and semi-fossorial locomotor ecologies. The ancestral nodes for Talpinae came up, as both fossorial and semi-fossorial, meaning the analysis was not able to determine one character state as the ancestral state for the subfamily.

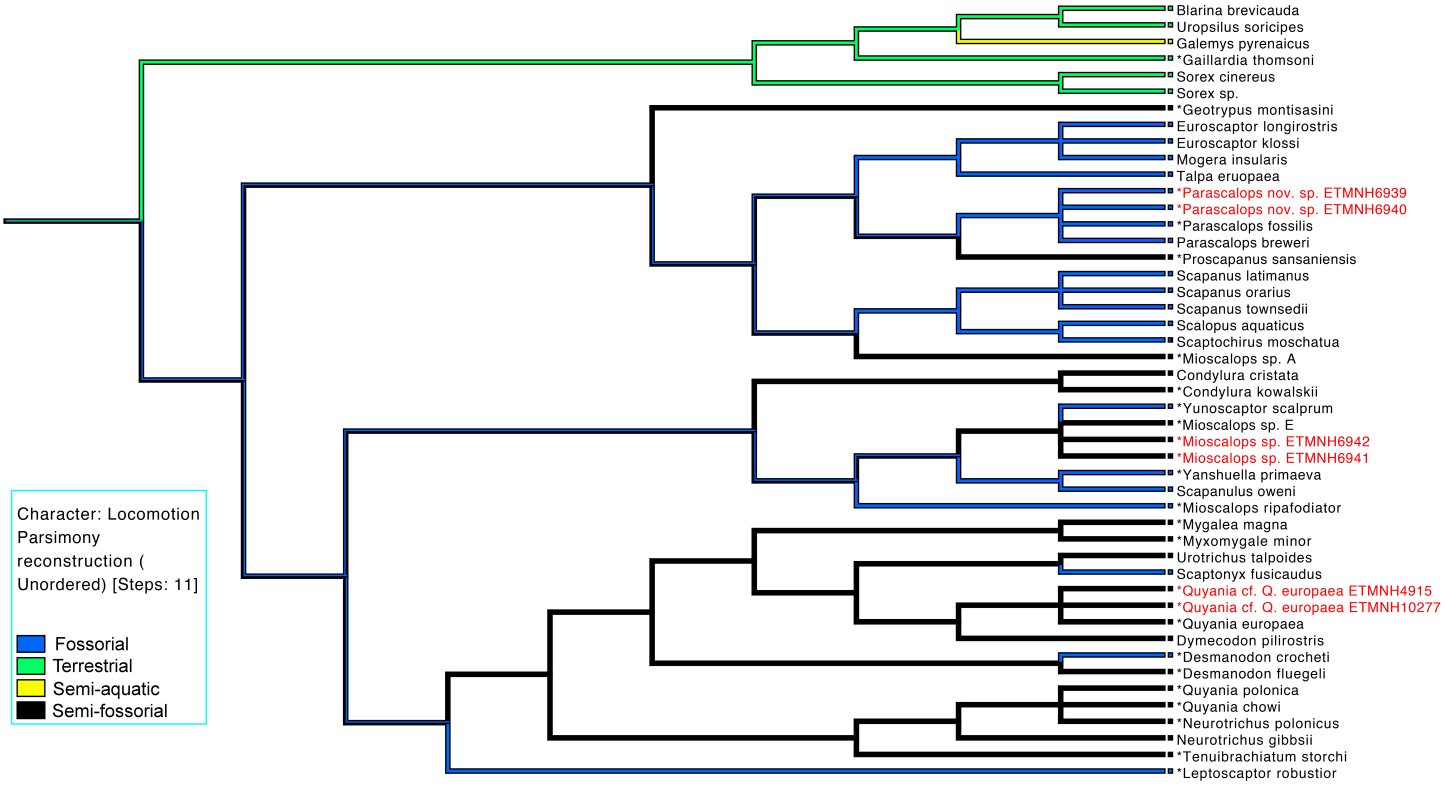

Figure 17: Ancestral state reconstruction of locomotor ecology. GFS taxa in red.

Finally, I looked at the dispersal events by plotting biogeographic ranges as continents onto the cluster analysis results (Figure 18). The dominant continents represented by this cluster analysis are Europe and North America. There are a few linages of Asian specific taxa, but they are not as common. Most of the clusters have a combination of European and North American taxa. There is only one cluster that occurs within a single continent and that is the Talpini, which are exclusively Eurasian. The analysis determined that the ancestral continent for the family Talpidae is Europe.

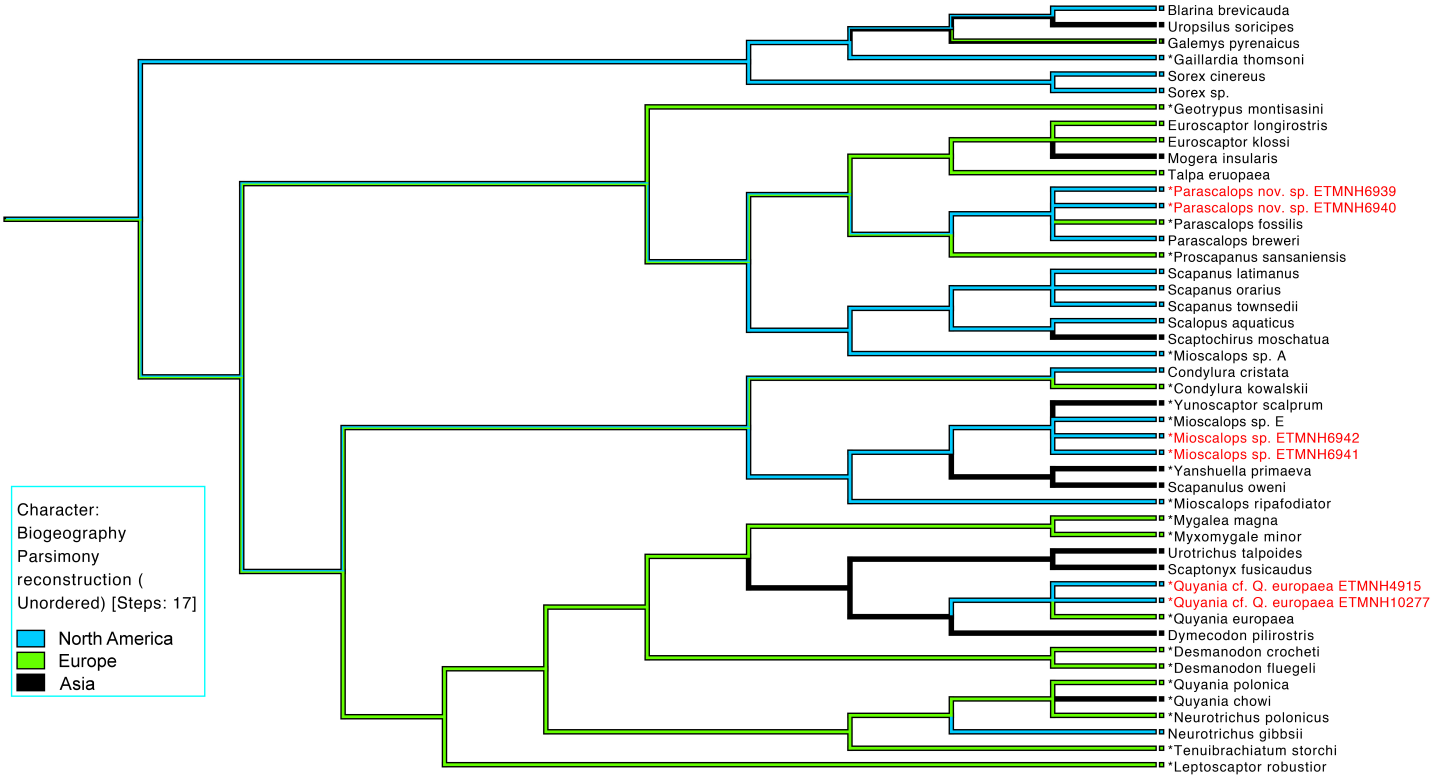

Figure 18: Ancestral state reconstruction of continent of origination. GFS taxa in red.

CHAPTER 5

DISCUSSION

Gray Fossil Site Ecology

At the Gray Fossil Site, there are at least four distinctly different talpids, each occupying a different ecological niche space. Not only is taxonomic diversity high, but also ecological diversity is higher than any other Pliocene-aged site in North America (Figure 8). There are no other fossil localities in North America that have this many ecologically distinct talpids.

Desmanini

Extant desmans are semi-aquatic moles that spend most of their life hunting and foraging underwater. They have long, laterally compressed tails fringed with stiff hairs to retain body heat (Nowak and Paradiso 1983; Palmeirim and Hoffmann, 1983; Gorman and Stone 1990). When swimming, they propel themselves with their hindlimbs, thus, have particularly heavily muscled hindlimbs and large, webbed hindfeet, when compared to other talpids (Palmeirim and Hoffmann 1983; Gorman and Stone 1990).

The desmans are specialized aquatic insectivores living in Eurasia today. The Russian desman, *Desmana moschata*, prefers slow moving streams, lakes, and ponds while the Pyrenean desman, *Galemys pyrenaicus*, requires fast-flowing, cold mountain streams and lakes with ample crustaceans and insect larvae (Nowak and Paradiso 1983; Palmeirim and Hoffmann 1983). *Galemys pyrenaicus* will seek shelter in the crevices between large rocks or small caves along the banks of rivers or take over the burrows of other animals. *Galamys* rarely digs its own burrow (Palmeirim and Hoffmann 1983). *Desmana moschata* will make nests on the shoreline under vegetation and roots above the high waterline. All entrances to their nests are only

accessible underwater (Palmeirim and Hoffmann 1983; MacDonald 1984). Both species occupy relatively shallow (0.5 - 2 m in depth), rocky-bottom water with ample spaces for invertebrates to hind in. (Palmeirim and Hoffmann 1983).

Having a Desmanini-like talpid at the Gray Fossil Site suggests that the paleosinkhole lake was a permanent, year-round lake that sustained year-round aquatic invertebrate populations. This is supported by the presence of fossil fish, neotenic salamanders, and beaver material at the site. If the fossil desman was behaviorally analogous with modern desmans, it would suggest that some parts of the paleosinkhole lake would likely have been relatively shallow (< 2 m in depth), as that is optimal foraging depth for extant desmans. The bottom of the lake would have been somewhat rocky with soft sediment for invertebrates to hind in. The edges of the lake could have had some rocks, a lot of low vegetation, or a combination of the two. The GFS desman likely would have nested close to the waters edge in either the thick vegetation or in void space between large enough rocks. The water at the edge of the lake would have been calm enough for fine sedimentation to take place and preserve microfossils, so it is unlikely that the desman material found here would be behaviorally analogous with *Galemys* or *Desmana*.

Parascalops

Extant *Parascalops breweri* (hairy-tailed mole) is a true fossorial mole, spending most, if not all, of its life completely underground; however, it will venture to the surface to move to a new area and to drink water. The extant species occupies a variety of rocky, gravelly, and sandy soils with deposits of interspersed clay in a variety of habitats ranging from large open fields to heavily wooded areas (Hallett 1978). *Parascalops breweri* is not known to permanently occupy places where the soil was very wet, areas where the soil had a heavy clay content, or areas on the summits of hills or ridges where the soil was hard, dry, sandy and without the protection of trees

or shrubs (Eadie 1939). They are known to eat just about any subterranean invertebrate that they come across while hunting in their tunnels (Eadie 1939; Hallett 1978).

Gray Fossil Site *Parascalops* nov. sp. is morphologically similar to, and found within the extant range of, the extant species and was similarly classified as fossorial by the canonical variates analysis. We have no definitive way of knowing how extinct animals behaved, but we can hypothesize an animal's ecology based on extant animal behavior, functional morphology, and localized paleoenvironments. Therefore, based on extant *Parascalops* behavior as well as lithological, floral, and pollen analyses of the Gray Fossil Site, suggests that GFS *Parascalops* was likely an exclusive burrower, and possibly burrowing in soil away from the lake's edge in the wooded areas, as this is where the ideal soil and food is for the extant species.

Mioscalops

Currently, there are no known extant relatives of this genus, but this is because we do not know how this taxon is related to any extant taxa. Based on the results of the hierarchical cluster analysis, the closest living relative could be *Condylura cristata* (star-nosed mole or *Scapanulus oweni* (Gansu mole), though *S. oweni* bears the greatest morphological resemblance.

Condylura cristata is a semi-fossorial and semi-aquatic talpid native to the eastern United States distributed as far north as Newfoundland and as far south as the Georgia-Florida boundary (Hamilton 1931; Petersen and Yates 1980). *Condylura cristata* is found in a variety of habitats, so long at the soil is moist. This species prefers to occupy areas of poor drainage, including both coniferous and deciduous forests, clearing, wet meadows, marshes, and peatlands (Hamilton 1931; Kurta 1995). *Condylura cristata* has also been found in the banks of streams, lakes and ponds (Hamilton 1931).

Scapanulus oweni is a semi-fossorial talpid endemic to China, in the provinces of Shaanxi, Gansu, Sichuan, Qinghai, and Hubei. This species is commonly found occupying the mossy undergrowth of montane fir forest (Smith and Xie 2008). Smith and Xie (2008) described *Scapanulus oweni* as being ecologically similar to *Scaptonyx fusicaudus* (long-tailed mole) as they overlap biogeographically and environmentally. Little is known about the ecology of *Scapanulus*, but it has been implied that it digs and maintains tunnels, like most fossorial moles, for food and shelter (Smith and Xie 2008).

Mioscalops is morphologically distinct from all living talpid taxa and its closest living relative is currently unknown, so inferring how GFS *Mioscalops* would have behaved here is dependent on ecomorphology. The canonical variates analysis classified GFS *Mioscalops* as both fossorial and semi-fossorial. This suggests that GFS *Mioscalops* could have been a successful burrower, but also may have been able to swim or move above ground with greater ease than most highly fossorial taxa. The hierarchical cluster analysis grouped GFS *Mioscalops* more closely with *Scapanulus oweni* and *Condylura cristata*, which further supports a generalized locomotor ecological classification for this taxon.

Quyania

Extant shrew moles are distinct from other moles. Their humeral morphology allows them to move above and below ground with little effort. Shrew moles are often mistaken for shrews as they bear striking resemblances, physically and ecologically, to one another. Some shrew moles (particularly *Neurotrichus*) are adept climbers, and will often climb into small bushes in search of food or a new nesting place (Dalquest and Orcutt 1942). Shrew moles are also great swimmers and use all four of their limbs plus their tail to move in the water (Carraway and Verts 1991; Abe et al. 2005). Shrew moles maintain burrows for nesting and hunting, but

they are far less complex than fossorial talpid burrows and often have open entrances that are easy to find (Dalquest and Orcutt 1942; Carraway and Verts 1991; Abe et al. 2005). Shrew moles often prefer soft soils that are very easy to dig in with plenty of organic matter. Shrew moles tend to be found in temperate rainforests, where the soil is soft and deep (Dalquest and Orcutt 1942; Ishii 1993), although some have been found in moist, weedy/brushy areas (Dalquest and Orcutt 1942).

The canonical variate analysis classified GFS *Q.* cf. *Q. europaea* as being semi-fossorial like most other extant shrew moles. This means that GFS *Q.* cf. *Q. europaea* could have been a soft soil digger like extant shrew moles. It may have also been able to climb small bushes to hunt or nest, and swim more efficiently than more specialized talpids. The hierarchical cluster analysis grouped GFS *Q.* cf. *Q. europaea* with the other extant shrew moles, specifically *Dymecodon pilirostris*, suggesting it is most morphologically similar to the extant shrew moles. Therefore, it is possible that GFS *Quyania* cf. *Q. europaea* behaved similarly to extant shrew mole. If GFS *Q.* cf. *Q. europaea* maintained burrows, they would probably be close the paleosinkhole lake's edge because there would be softer and moister soil closer to the water.

Biogeography

Historically, North America and Europe have had the highest diversity of talpids through geologic time (Gunnell et al. 2008). Peak taxonomic diversity and biogeographical distributions occurred during the middle Miocene (Hutchison 1968; Gorman and Stone 1990; Gunnell et al. 2008). The GFS is unique because it has high talpid diversity, both in terms of the number of taxa present but also ecologically, at a point in geologic time when talpid diversity was on the decline worldwide. The number, and ecological diversity, of talpid taxa found at the GFS was

unexpected; however, taxonomic occurrences of extant genera were expected because similar patterns are evident at other Blancan-aged sites.

GFS *Parascalops* nov. sp. is within the extant range of the living species (Eadie 1939). This means that *P.* nov. sp. was occupying the same parts of the United States approximately 5 million years ago because the eastern United States has historically been forested throughout the Cenozoic (Wolfe 1975; Guo 1999). The genus was widespread during the early Pliocene – Pleistocene (Figure 20), getting as far north as New England in North America. The extant species, *Parascalops breweri*, is only known from North America, but a fossil species, *P. fossilis*, has been found in Europe.

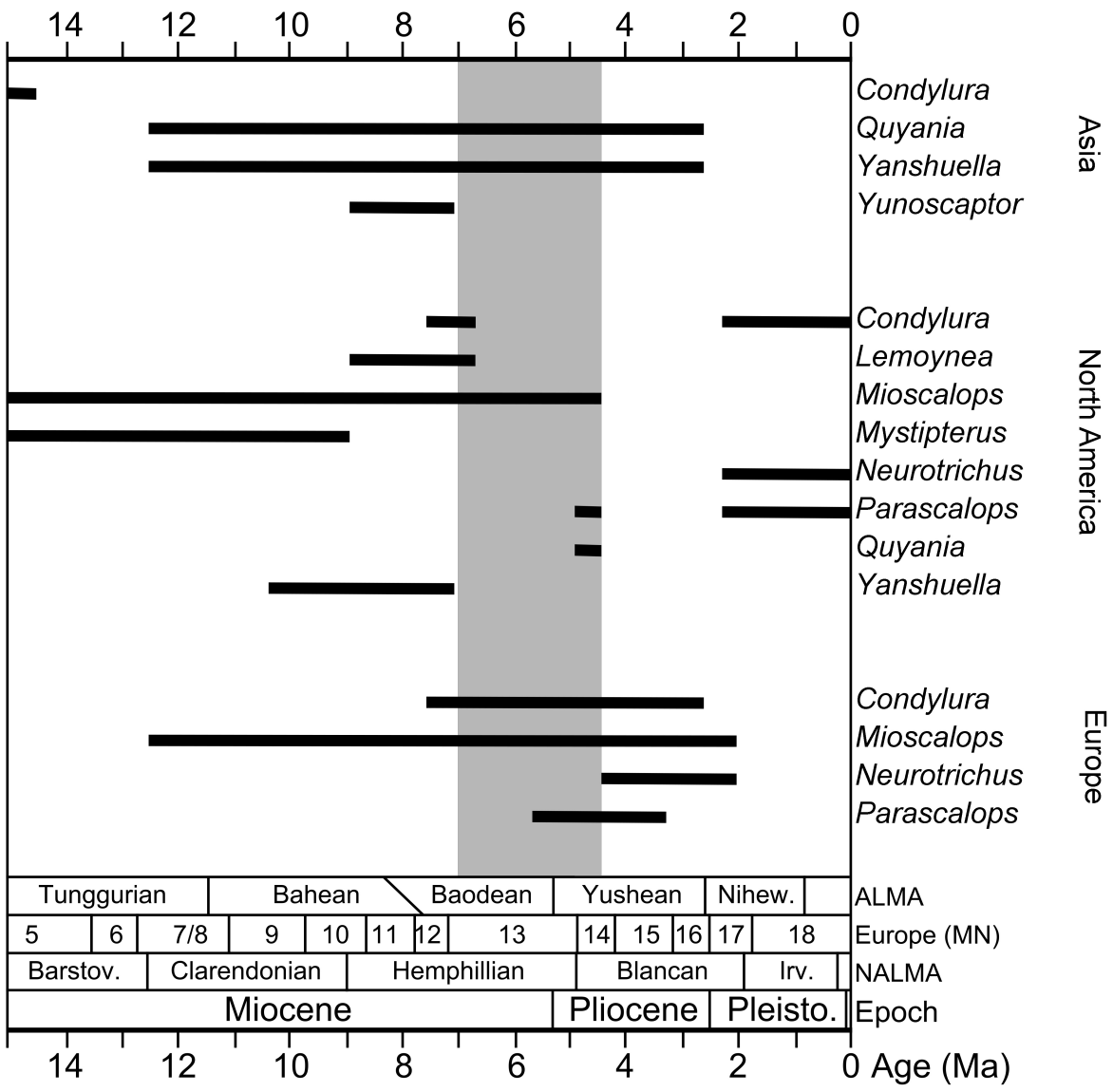

Figure 19: Biostratigraphic ranges of GFS taxa and morphologically similar talpids. Age of the Gray Fossil Site in gray.

Mioscalops was spatially and temporally widespread (Figure 20) in comparison to other talpid taxa. Its more generalized humerus morphology allowed it to occupy available niche spaces in more places than specialized taxa; therefore, finding *Mioscalops* at the Gray Fossil Site was not surprising. What is unusual is the lack of *Mioscalops* occurrences that have been noted in the southeastern United States. Part of this is due to the lack of fossil sites being found in this

part of the United States, but also because researchers have not identified their talpid material past the family level (Gunnell et al. 2008).

Quyania is known from Mio-Pliocene of China and Europe (Figure 20), and may be known from western North America. Material previously described by Hutchison (1968) as ?*Neurotrichus polonicus* has a striking morphological resemblance to *Quyania polonica* (Rzebik-Kowalska 2014). The cluster analysis results grouped ?*Neurotrichus polonicus* with *Quyania chowi* and *Quyania polonica*, providing further evidence that ?*N. polonicus* may be *Q. polonica*. Finding *Quyania* in Europe, Asia, and western North America supports GFS *Quyania* being a valid identification. GFS material was identified, as *Quyania* cf. *Q. europaea*, which makes this the first occurrence of this species outside of Eurasia, but not the first occurrence of the genus.

The extant tribe, Desmanini, currently has two living members, *Galemys pyrenaicus* and *Desmana moschata*. Both taxa are found exclusively in Eurasia. Fossil desmanine talpids have been found all over Eurasia throughout the Oligo-Miocene, with peak diversity during the Pliocene of Europe, but a few taxa have been found in North America (Figure 20). One taxon is *Lemoynea*, which was found in the late Miocene of Nebraska (Brown 1980). Since this discovery, no other true desmanine taxa have been found in North America. Many taxa were once called Desmanini, but they all lack the synapomorphies that make them true desmans. The GFS Desmanini? material represents stem desmans outside the crown clade, but related to the evolutionary lineage leading to extant desmans.

The talpid occurrences at the Gray Fossil Site are quite unique. They represent first or oldest occurrences of mostly Eurasian taxa. Which raises the question of when and how did they get here? Numerous studies (Sher 1999; Flynn et al. 2003; Vila et al. 2011; Guo et al. 2012; Konidaris et al. 2014) have shown that the Beringia Landbridge was open during the Mio-

Pliocene and was actively used by taxa to migrate between the New and Old Worlds. It is likely that talpids were also using this pathway to move from Eurasia to and from North America (Figure 18). Particular tribes, like the Condylurini and the Scalopini, are known to originate in North America, but fossil forms are found in Europe, thus indicating that these taxa had to get from North America to Europe after the Oligocene, but before the middle Pliocene in order for the timing of their occurrence in Eurasia.

Canonical Variate Analysis

The CVA classified all talpid taxa into 1 of 4 locomotor ecologies. The analysis correctly classified locomotor groups in 99.2% of original grouped cases and 95.5% when cross-validated. This means that the analysis was successfully able to correctly classify taxa with known locomotor ecologies as such.

Over half (n=17) of the fossil taxa were classified as semi-fossorial. The semi-fossorial locomotor ecology is the broadest ecological category included in this analysis. It includes any talpid species that is not an ecological specialist, such as being fully fossorial, fully terrestrial, or semi-aquatic. Being such a broad ecological category, there is a lot of morphological variation being represented by this group. Most of the fossil taxa classified as semi-fossorial because it encompasses the greatest amount of the shape variation, thus the analysis has an easier time grouping taxa into this category using the shape data (principle warps and uniform components).

There were a few fossil taxa that classified as semi-aquatic (n = 1) and terrestrial (n = 2). The single taxon that classified as semi-aquatic was *Mygalea magna*†, an early Miocene-aged (early Hemingfordian NALMA, MN 3 ELMA) desman from the Czech Republic (Van den Hoek Ostende and Fejfar 2006). The two taxa that classified as terrestrial are *Desmanella gudrunae*†, an early Miocene-aged (early Hemingfordian, MN 3) uropsiline shrew mole from the Czech

Republic (Van den Hoek Ostende and Fejfar 2006), and *Gaillardia thompsoni*†, a late Miocene-aged (latest Hemphillian) desman from Oregon, New Mexico, and Nebraska (Martin 2017). *Mygalea magna*† classified as semi-aquatic, but its position in morphospace is closer to the terrestrial ecological group. Both *Desmanella gudrunae*† and *Gaillardia thompsoni*† classified as terrestrial, but *G. thompsoni*† is positioned more closely to the semi-aquatic ecological group. All 3 of these taxa were well outside their respective locomotor ecology morphospace groupings, but still classified as such. This implies that these taxa might possibly have been proficient in a few different locomotor ecologies, or I do not have enough data in this analysis for it effectively separate individual taxa and to make better, more consistent groupings.

The GFS taxa all had relatively low conditional probabilities, but high posterior probabilities. This indicates that the GFS taxa will always classify as a particular locomotor ecology (high posterior probability), but it is unlikely that this particular outcome will happen again (low conditional probability). The GFS specimens may appear morphologically similar to extant taxa with known locomotor ecologies, but the cluster analysis results suggest that the GFS taxa were moving and behaving differently from extant analogous forms. Even though GFS *Quyania* cf. *Q. europaea* classified as semi-fossorial, GFS *Mioscalops* sp. classified as both semi-fossorial and fossorial, and GFS *Parascalops* nov. sp. classified as fossorial, these taxa were probably not behaving analogously to extant taxa. It is possible that the GFS taxa represent some of the most specialized talpid taxa during the Mio-Pliocene, as we do not have a strong fossil record for talpid locomotor ecological specialization during this time period, but in comparison to extant specialized taxa, they appear less ecologically specialized. This hypothesis is supported by the intermediate positions for the GFS taxa in morphospace.

Hierarchical Cluster Analysis

In contrast to morphological phylogenetics cladograms, both the individuals' and average position trees represent phenograms that represent morphological similarity, but also take ecological convergence into consideration. Geometric morphometrics were used to capture overall shape variation in taxa and examine how morphology reflected ecology. Variables identified as characteristics of ecology in the CVA were removed to limit some of the convergent ecological signal notorious for creating most of the problems in traditional morphological phylogenetics of talpids.

For the most part, the cluster analysis effectively removed the influence of locomotor convergence (Figures 14 and 15). There are four distinct clusters (Condylurini, shrew moles, Scalopini, and Talpini), with two more groups (Desmanini and Uropsilinae) lumped into the outgroup (Soricidae). Each group created by the cluster analysis contains the taxa originally hypothesized to be apart of that group. Also, every taxon's position in the cluster analysis can be explained and justified using traditional systematics. What this means is that humerus morphology can be used to evaluate the evolutionary relationships at the family level once ecological convergence is partially removed from an analysis.

The Gray Fossil Site taxa clustered into 3 different groups (Figure 15) representing 3 distinctly different locomotor ecologies. Each of the GFS taxa were placed into clusters with extant and other fossil taxa that share the most morphological similarities. GFS *Parascalops* nov. sp. clustered with all individuals in the genus *Parascalops*, which includes extant *P. breweri* and *P. fossilis*†, along with *Proscapanus sansansiensis*†. Having all the *Parascalops* individuals cluster together means that there were enough morphological similarities between the extant individuals, other fossil individuals, and the GFS individuals for them to be grouped together.

The combination of the GFS *P.* nov. sp., extant *P. breweri*, *Proscapanus sansansiensis*†, and the other highly fossorial North American taxa (*Scapanus latimanus*, *Scapanus orarius*, *Scapanus townsedii*, *Scalopus aquaticus*, *Scaptochirus moschatua*, and *Mioscalops* sp. A†) make up the Scalopini cluster. This cluster is very similar to the molecular phylogeny generated by He et al. (2016) with the exceptions of *Scapanulus oweni*, which was placed into the Condylurini cluster, being excluded and *Scaptochirus moschatua* being included. Morphologically and ecologically, this grouping makes sense. All of the taxa included in this Scalopini cluster are highly fossorial specialists, while *Scapanulus* is considered to be more semi-fossorial. *Scapanulus* morphology is most similar to that of *Condylura*, so it makes sense that they would cluster together.

GFS *Quyania* cf. *Q. europaea* clustered with the other *Q. europaea*† and extant *Dymecodon pilirostris*. The GFS material clustered with the European occurrence of *Q. europaea*, which supports calling them all *Q. europaea*. Interestingly, both GFS *Q.* cf. *Q. europaea* and other *Q. europaea* did not cluster with either of the other species of *Quyania*. The two other species of *Quyania* (*Q. chowi* and *Q. polonica*) clustered with *Neurotrichus polonica* and *Neurotrichus gibbsii*; however, the *Neurotrichus* cluster is depicted as being the ancestral group to the *Q. europaea* cluster. This is interesting because it implies that the *Neurotrichus* lineage diverged much earlier that previously thought (Storch and Qui 1983) in comparison to *Quyania*, *Urotrichus*, or *Dymecodon*. Morphologically, all of these taxa have relatively gracile humeri with minimal adaptations for fossorial life. From an ecological perspective, these taxa are semi-fossorial generalists capable of burrowing, swimming, or walking above ground with ease. It makes sense morphologically and ecologically that all of these taxa would be grouped together. Also, this general grouping matches the He et al. (2016) phylogeny.

GFS *Mioscalops* clustered with *Mioscalops* sp. E†, *Yunoscaptor scalprum*†, *Yanshuella primaeva*†, *Scapanulus oweni*, *Mioscalops ripafodiator*†, *Condylura kowalskii*†, and *Condylura cristata*, which make up the Condylurini cluster. Interestingly, the cluster analysis grouped GFS *Mioscalops* more closely with *Yunoscaptor scalprum* and *Mioscalops* sp. E, implying that there is a closer relationship between these taxa. There was also distinct separation between *Yunoscaptor* and *Yanshuella*, and the placement of *Mioscalops ripafodiator* was quite surprising. Previous studies (Storch and Qui 1983; 1991) have suggested that *Yunoscaptor* and *Yanshuella* were more closely related because most species within each genus existed in similar places at the same time, so having them separate in this cluster analysis was unexpected; however, a single species of *Yanshuella* has been found in North America, *Y. columbiana*, and it is morphological similar to *Neurotrichus gibbsii* (Hutchison 1968; Storch and Qui 1983; Carraway and Verts 1991), *Condylura cristata*, and *Scapanulus oweni*. *Mioscalops ripafodiator* has been described as being relatively specialized for a generalist taxon (Hutchison 1968). It did not group with any of the other four taxa included in this analysis that share the same genus. One reason why these taxa could be separated is due to the lack of intraspecific variation in each genus, but it could also be due to incorrect classification. There were enough morphological distinctions between these *Mioscalops* taxa that the cluster analysis determined them to be separate. Morphologically, all of the taxa classified in the Condylurini cluster have longer and less robust humeri compared to the more fossorial specialists, though these humeri are not nearly as gracile as those of the shrew mole cluster. Condylurine talpids are still efficient burrowers, but not sufficiently adept for a completely underground lifestyle. Ecologically, the taxa included in this grouping were semi-fossorial generalist talpids that could have been good at swimming, but were likely not adept at walking above ground.

The positions of the clusters generated in this analysis are relatively similar to those in the He et al. (2016) phylogeny. On the He et al. (2016) cladogram, the Uropsilinae is the most ancestral cluster, followed by the Scalopini, then the shrew mole clusters, and finally the Condylurini, Desmanini, and Talpini clusters. Condylurini and Desmanini are drawn as sister clusters and the Talpini tribe as the sister cluster to them.

In this cluster analysis, two of the six clusters (Uropsilinae and Desmanini) are nested in the outgroup. The Scalopini tribe is the first totally separate cluster and was drawn as the most ancestral clusters with the Talpini tribe nested within it. The He et al. (2016) phylogeny shows the best separation between these two clusters; however, there is weak statistical confidence supporting the position for the tribe Talpini. In this cluster analysis, there were not enough landmark differences and individuals to completely separate these groups; although, most of the species belonging to each tribe did cluster together. Finally, the shrew mole cluster and Condylurini cluster are depicted as being sister clusters to each other, with a shared ancestor linking them to the Scalopini group.

Even though I applied an ecological correction to the data before performing the hierarchical cluster analysis, there was still a strong ecological signal influencing the clusters. One reason why there could still be so much ecological influence is because of the evolutionary history of talpid humerus specialization. Locomotor specialization is likely what drove the change in humerus shape, thus the entire structure exists because of the evolutionary selective forces driving the shape of the humerus.

A minor issue with this hierarchical cluster analysis is the lack of intraspecific variation due to small sample sizes. In the individuals' phenogram, a single individual represents several entire clusters, such as in the Urotrichini and Uropsilinae. Also, a limited number of characters

does not give the analysis enough points of reference to find similarities or differences between humerus shapes, thus creating less informed clusters. To effectively separate all taxa and resolve polytomies, there needs to be more characters (number of landmarks) than taxa. A prime example of this is the outgroup for both the individuals' and species mean phenograms (Figure 12 and 13). *Uropsilus*, *Galemys*, and *Gaillardia*† were grouped with Soricidae (true shrews). Morphologically, all of these taxa are relatively similar looking with elongated humeral shafts and reduced proximal ends, thus the cluster analysis grouped them together. With respect to their DNA, these taxa are more distantly related to one another, but small sample sizes, limited character sampling, and similar morphology is causing these taxa to be grouped together.

Although convergence and limited character sampling have negatively affected the resolution of the cluster analysis, the hierarchical cluster analysis worked fairly well, and allows new interpretations to be made about the history of the family.

Ancestral State Reconstruction

Ancestral state reconstructions are a powerful tool for visualizing changes in traits across a lineage, but also for determining the ancestral state of a particular character. In this case, ancestral state reconstructions were used to evaluate evolutionary trends at the family level. Based on the results from the ancestral state reconstructions, the ancestral state for the most basal members of the family Talpidae would have had a humerus length between 10 and 12 mm long. Ecologically, the ancestral state talpid would have been semi-fossorial or fossorial from Europe.

The results of the ancestral state reconstructions were not quite as expected. Predicted ancestral humerus length was surprisingly large (Figure 16) and the predicted ancestral locomotor ecology was much more specialized (Figure 17) than what was expected for the ancestral state condition. When compared to the He et al. (2016) study, there was a much smaller

predicted ancestral humerus length (Figure 21) and more generalized locomotor ecology (Figure 22) than were found using the hierarchical cluster analysis for ancestral state reconstruction. Past literature (Hutchison 1968; 1974; Gunnell et al. 2008) suggests that the ancestral body size and morphology of talpids would have been small, more like that of modern shrews. Even though the oldest talpids are distinctly talpid-looking, they appear more like generalist (i.e. gracile, reduced distal and proximal ends, long diaphysis, etc.) in contrast to their specialized descendants. The main reason why I got this result is because of how the clusters were structured in Mesquite. The ancestral condition will change at nodes based on where and how the lineages are positioned on the phenogram. The outgroup cluster in this analysis contains two of the largest extant and extinct talpids included in the analysis, thus increasing the hypothesized ancestral size for the family. Therefore, it is likely that I am getting such a large ancestral humerus length because of how my clusters are structured.

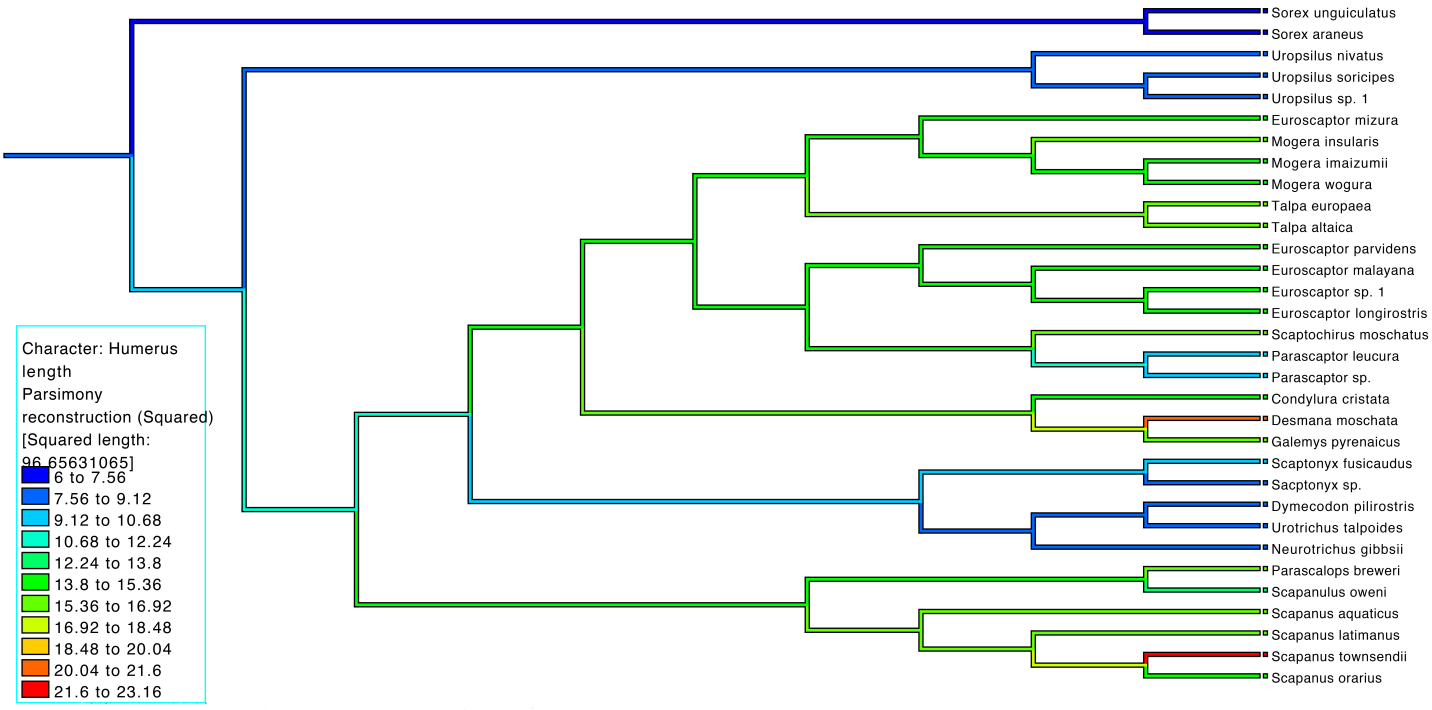

Figure 20: Ancestral state reconstruction of body size using humerus length plotted on the He et al. (2016) phylogeny.

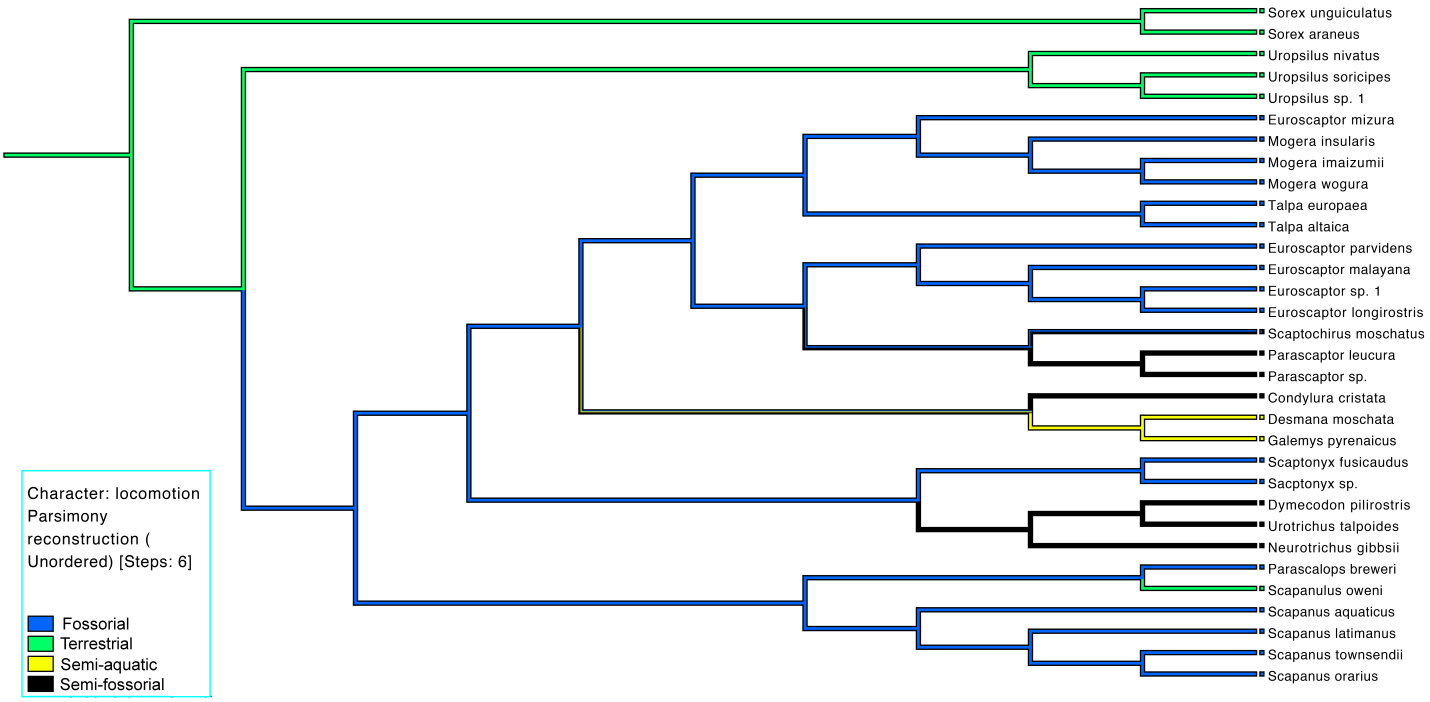

Figure 21: Ancestral state reconstruction of locomotor ecology plotted on the He et al. (2016) phylogeny.

The fossil record and He et al. (2016) phylogeny (Figure 23) have suggested that Asia was likely the site of talpid origination (Gunnell et al. 2008), but the results from this analysis suggest that the ancestral place of origination is in Europe (Figure 18). One reason why I could be getting this result is because of how many more European and North American taxa are in this analysis. This analysis is heavily weighted in favor of North American and European taxa. Another reason could be due to taxonomic positions on the phenogram. Mesquite will change the weighting of certain characters based on where a particular taxon falls within a cluster. Therefore, increasing taxonomic representation and species sample sizes would improve the cluster analysis resolution, but also give more accurate ancestral state reconstruction hypotheses.

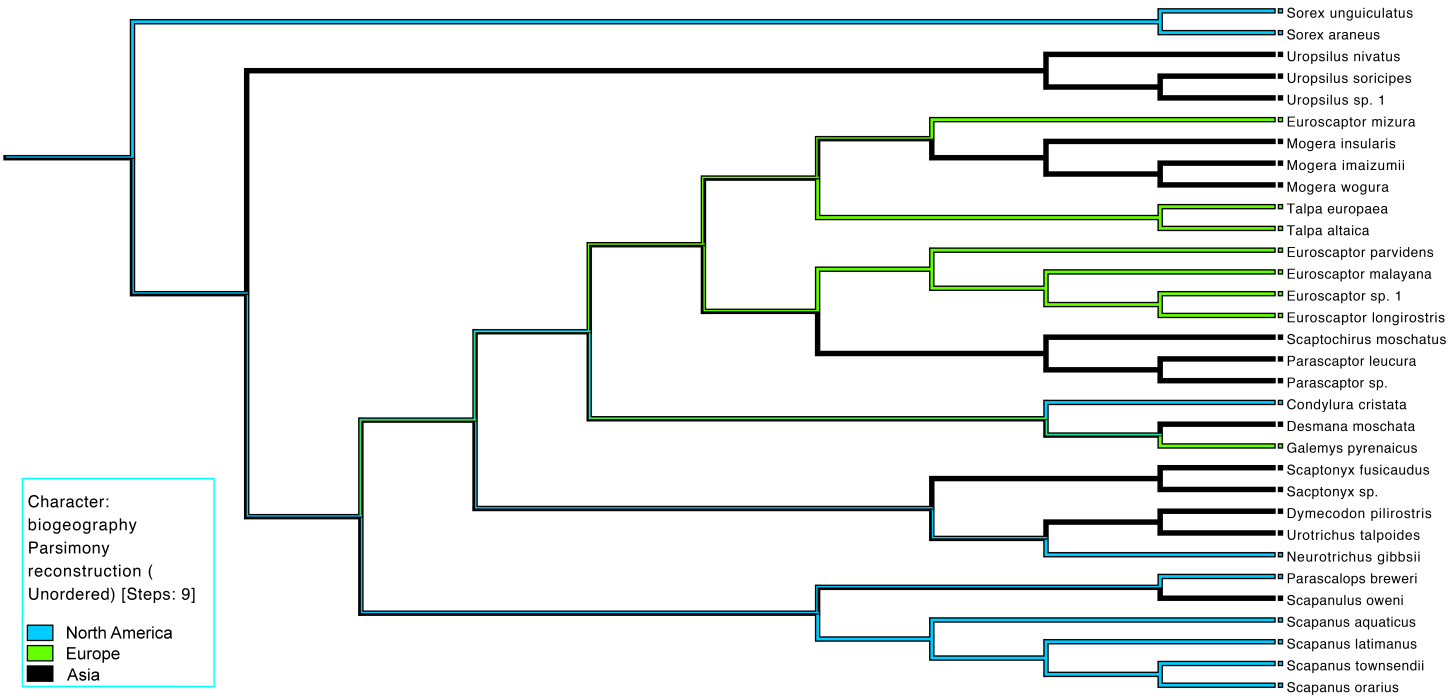

Figure 22: Ancestral state reconstruction of continent of origin plotted on the He et al. (2016) phylogeny.

Looking at the predictions for the GFS taxa, they follow the trends of the other taxa in their cluster; they have the same humerus lengths, utilize the same locomotor ecologies, and are found on the same continents. These taxa are ecologically distinct from one another, and also validate the current taxonomic identification placed on each taxon.

CHAPTER 6

CONCLUSIONS

The Gray Fossil Site has a new fossil talpid assemblage unlike any seen in North America before. There are at least 4 talpid taxa present at the site and they represent 4 distinct locomotor ecologies each requiring a different niche space. GFS *Parascalops* nov. sp. is a typical fossorial talpid and morphologically similar to the extant species making this the oldest occurrence of the genus globally. GFS *Mioscalops* is a semi-fossorial talpid found in both Europe and North America, but this is the first occurrence in the southeastern United States. GFS *Quyania* cf. *Q. europaea* is a semi-fossorial shrew mole known from the Pliocene of Europe, making this the first occurrence of the species outside of Europe. The tribe Desmanini is well known from the fossil record of Eurasia, but very few specimens have been found in North America. The GFS specimens represent stem desmans and are the first of their kind found in North America.

Geometric morphometric analyses showed that humerus shape is highly reflective of locomotor ecology in extant and fossil talpids. Through hierarchical cluster analysis, that data was also used to secondarily verify taxonomic designations for the GFS taxa. Even though convergence and limited sampling of variables affected how well the morphological cluster analysis was able perform, it did largely recreate the relationships found in the most recent molecular cladogram (He et al. 2016). All six tribes were represented on the cluster analysis phenograms, all of the shrew moles (Scaptonychini, Urotrichini, and Neurotrichini) clustered together, and there was some separation between the tribes Talpini and Scalopini. Additionally, the cluster analysis provides new information about the placement of fossil taxa and which parts of the tree still need better resolution.

REFERENCES

Abe H, Ishii N, Ito T, Kaneko Y, Maeda K, Miura S, Yoneda M. 2005. *A Guide to the Mammals of Japan*. Tokai University Press, Kanagawa, Japan.

Bannikova AA, Zemlemerova ED, Lebedev VS, Aleksandrov DY, Fang Y, Sheftel BI. 2015. Phylogenetic position of the Gansu mole *Scapanulus oweni* Thomas, 1912 and the relationships between strictly fossorial tribes of the family talpidae. *Dokl Biol Sci*. 464:230–234.

Boardman GS, Schubert BW. 2011. First Mio-Pliocene salamander fossil assemblage from the southern Appalachians. *Palaeontologia Electronica.* 14(2): p.16A.

Bourque JR, Schubert BW. 2015. Fossil musk turtles (Kinosternidae, Sternotherus) from the late Miocene–early Pliocene (Hemphillian) of Tennessee and Florida. *Journal of Vertebrate Paleontology*. 35(1):p.e885441.

Bown TM. 1980. The fossil Insectivora of Lemoyne Quarry (Ash Hollow Formation, Hemphillian), Keith County, Nebraska. *Transactions of the Nebraska Academy of Sciences and Affiliated Societies*. 284.VIII: 99-122.

Brandon S. 2013. Discovery of bald cypress fossil leaves at the Gray Fossil Site, Tennessee and their ecological significance. Undergraduate honors thesis, East Tennessee State University.

Cabria MT, Rubines J, Gomez-Moliner B, Zardoya R. 2006. On the phylogenetic position of a rare Iberian endemic mammal, the Pyrenean desman (*Galemys pyrenaicus*). *Gene* 375:1–13.

Campbell B. 1939. The shoulder anatomy of the moles. A study in phylogeny and adaptation. *Developmental Dynamics*, 64(1), 1-39.

Carrasco MA, Barnosky AD, Kraatz BP, Davis EB. 2007. The Miocene mammal mapping project (MIOMAP): an online database of Arikareean through Hemphillian fossil mammals. *Bulletin of the Carnegie Museum of Natural History.* 39:183-188.

Carraway LN, Verts BJ. 1991. Neurotrichus gibbsii. *Mammalian Species*, (387), 1-7.

Dalquest WW, Orcutt DR. 1942. The biology of the least shrew-mole, Neurotrichus gibbsii minor. *The American Midland Naturalist*, *27*(2), 387-401.

DeSantis LR, Wallace SC. 2008. Neogene forests from the Appalachians of Tennessee, USA: geochemical evidence from fossil mammal teeth. *Palaeogeography, Palaeoclimatology, Palaeoecology*. 266(1):59-68.

Douady CJ, Chatelier PI, Madsen O, de Jong WW, Catzeflis F, Springer MS, Stanhope MJ. 2002. Molecular phylogenetic evidence confirming the Eulipotyphla concept and in support of hedgehogs as the sister group to shrews. *Molecular phylogenetics and evolution*, 25(1), 200-209.

Eadie WR. 1939. A contribution to the biology of Parascalops breweri. *Journal of Mammalogy*, *20*(2), 150-173.

Flynn LJ, Tedford RH, Novacek MJ, Woodburne MO, Hunt Jr RM, Gould GC, Adam PJ. 2003. Vertebrate fossils and their context: contributions in honor of Richard H. Tedford. Bulletin of the AMNH; no. 279.

Fortelius M. 2013. New and Old Worlds Database of Fossil Mammals (NOW). University of Helsinki. *Available at http://www.helsinki.fi/science/now/* (Accessed 10 August 2017).

Freeman A. 1886. The anatomy of the shoulder and upper arm of the mole (*Talpa europaea*). *Journal of Anatomy and Physiology*, 20, 201-219.

Gambaryan PP, Gasc JP, Renous S. 2002. Cinefluorographical study of the burrowing movements in the common mole, Talpa europaea (Lipotyphla, Talpidae). *Russian Journal of Theriology*, *1*(2), 91-109.

Gong F, Karsai I, Liu YSC. 2010. Vitis seeds (Vitaceae) from the late Neogene Gray fossil site, northeastern Tennessee, USA. *Review of Palaeobotany and Palynology*, *162*(1), 71-83.

Gorman ML, Stone RD. 1990. The Natural History of Moles. Ithaca, New York, Comstock Publishing Associates.

Graham RW, Lundelius Jr EL. 2010. FAUNMAP II: New Data for North America with a Temporal Extension for the Blancan, Irvingtonian and early Rancholabrean. FAUNMAP II Database, version 1.0. *Available at http://www.ucmp.berkeley.edu/faunmap* (Accessed 10 August 2017).

Guo Q. 1999. Ecological comparisons between Eastern Asia and North America: historical and geographical perspectives. *Journal of Biogeography*, *26*(2), 199-206.

Guo P, Liu Q, Xu Y, Jiang K, Hou M, Ding L, Pyron RA, Burbrink FT. 2012. Out of Asia: natricine snakes support the Cenozoic Beringian dispersal hypothesis. *Molecular Phylogenetics and Evolution*, *63*(3), 825-833.

Gunnell GF, Bown TM, Hutchison JH, Bloch JI. 2008. Chapter 7: Lipotyphla, in Janis CM, Gunnell GF, Uhen MD. (eds.) Evolution of Tertiary Mammals of North America:. Cambridge University Press, 89 – 126.

Hallett JG. 1978. Parascalops breweri. *Mammalian Species*, (98), 1-4.

Hamilton WJ. 1931. Habits of the star-nosed mole, *Condylura cristata*. *Journal of Mammalogy*, *12*(4), 345-355.

He K, Shinohara A, Jiang XL, Campbell KL. 2014. Multilocus phylogeny of talpine moles (Talpini, Talpidae, Eulipotyphla) and its implications for systematics. *Molecular Phylogenetics and Evolution*, *70*, 513-521.

He K, Shinohara A, Helgen KM, Springer MS, Jiang XL, Campbell KL. 2016. Talpid mole phylogeny unites shrew moles and illuminates overlooked cryptic species diversity. *Molecular Biology and Evolution*, msw221.

Hildebrand M. 1974. Analysis of the Vertebrate Structure. John Wiley and Sons, New York, London, Sidney, Toronto. 1st edition.

Hugueney M. 1972. Les talpidés (Mammalia, Insectivora) de Coderet-Bransat (Allier) et l'évolution de cette famille au cours de l'Oligocene supérieur et du Miocene inférieur d'Europe, Docum. Lab. Géol. Fac. Sci. Lyon, no. 50, 1–81.

Hutchison JH. 1968. Fossil Talpidae (Insectivora, Mammalia) from the later Tertiary of Oregon. *Bulletin of the Museum of Natural History University of Oregon* 11:1–117.

Hutchison JH. 1974. Notes on type specimens of European Miocene Talpidae and a tentative classification of old world Tertiary Talpidae (Insectivora: Mammalia). *Geobios* 7:211–256.

Hutchison JH. 1984. Cf. Condylura (Mammalia: Talpidae) from the late Tertiary of Oregon. *Journal of Vertebrate Paleontology*, *4*(4), 600-601.

Hutchison JH. 1987. *Late Pliocene (Blancan) Scapanus (Scapanus)(Talpidae: Mammalia) from the Glenns Ferry Formation of Idaho*. Museum of Paleontology, University of California.

Hutterer R. 1995. *Archaeodesmana* Topachevski & Pashkov, the correct name for *Dibolia* Rümke, a genus of fossil water mole (Mammalia: Talpidae). *Bonn. Zool Beitr.* 45:3-4,171-172.

Hutterer R. 2005. Order Soricomorpha. In: Wilson DE, Reeder DA, editors. *Mammal Species of the World: A Taxonomic and Geographic Reference*. Baltimore: John Hopkins University Press. p. 220–311.

IBM Corp. Released 2013. IBM SPSS Statistics for Windows, Version 25.0. Armonk, NY: IBM Corp.

Ishii N. 1993. Size and distribution of home ranges of the Japanese shrew-mole *Urotrichus talpoides*. *Journal of the Mammalogical Society of Japan* 18: 87-98.

Jasinski SE. 2013. Fossil *Trachemys* (Testudines: Emydidae) from the Late Hemphillian of Eastern Tennessee and its implications for the evolution of the Emydidae. MS thesis, East Tennessee State University.

Klietmann J, Nagel D, Rummel M, Van den Hoek Ostende LW. 2015. A gap in digging: the Talpidae of Petersbuch 28 (Germany, Early Miocene). Paleaontologische Zeitschrift 89:563–592.

Konidaris GE, Roussiakis SJ, Theodorou GE, Koufos GD. 2014. The Eurasian occurrence of the shovel-tusker *Konobelodon* (Mammalia, Proboscidea) as illuminated by its presence in the late Miocene of Pikermi (Greece). *Journal of Vertebrate Paleontology*, *34*(6), 1437-1453.

Koyabu D, Endo H, Mitgutsch C, Suwa G, Catania KC, Zollikofer CP, Sánchez-Villagra MR. 2011. Heterochrony and developmental modularity of cranial osteogenesis in lipotyphlan mammals. *EvoDevo*, *2*(1), 21.

Kretzoi M, Kretzoi M. 2000. Fossilium catalogus 1: Animalia. *Index Generum et Subgenerum Mammalium. Backhuys Publ., Leiden*.

Kurta A. 2017. *Mammals of the Great Lakes region*. University of Michigan Press.

MacDonald D. 1984. *The Encyclopedia of Mammals*. Facts on File. Inc, New York. p.766-769.

Maddison WP, Maddison DR. 2018. Mesquite: a modular system for evolutionary analysis. Version 3.40. http://mesquiteproject.org

Martín-Suárez E, Bendala N, Freudenthal M. 2001. *Archaeodesmana baetica*, sp. nov. (Mammalia, Insectivora, Talpidae) from the Mio–Pliocene transition of the Granada Basin, southern Spain. *Journal of Vertebrate Paleontology*, *21*(3), 547-554.

McKenna MC, Bell SK. 1997. Classification of mammals: above the species level. New York: Columbia University Press.

Mead JI, Schubert BW, Wallace SC, Swift SL. 2012. Helodermatid lizard from the Mio-Pliocene oak-hickory forest of Tennessee, eastern USA, and a review of monstersaurian osteoderms. *Acta Palaeontologica Polonica.* 57:111-121.

Meier PS, Bickelmann C, Scheyer TM, Koyabu D, Sánchez-Villagra MR. 2013. Evolution of bone compactness in extant and extinct moles (Talpidae): exploring humeral microstructure in small fossorial mammals. *BMC evolutionary biology*, *13*(1), 55.

Miller GS. 1912. *Catalogue of the mammals of western Europe:(Europe exclusive of Russia) in the collection of the British Museum*. Order of the Trustees. British Museum (Natural History), London, 1019 pp.

Motokawa M. 2004. Phylogenetic relationships within the family Talpidae (Mammalia: Insectivora). *Journal of Zoology*. 263:147–157.

Nowak RM, Paradiso JL. 1983. *Walker's Mammals of the World,* 4th ed., Vol. I. Baltimore, Johns Hopkins University Press.

The NOW Community 2017. New and Old Worlds Database of Fossil Mammals (NOW). Licensed under CC BY 4.0. Release 23 Feb 2012, retrieved 20 Feb 2017 from http://www.helsinki.fi/science/now/.

Ochoa D, Whitelaw M, Liu YS, Zavada M. 2012. Palynology from Neogene sediments at the Gray Fossil Site, Tennessee, USA: Floristic implications. *Review of Palaeobotany and Palynology*. 184:36-48.

Ochoa D, Zavada MS, Liu Y, Farlow JO. 2016. Floristic implications of two contemporaneous inland upper Neogene sites in the eastern US: Pipe Creek Sinkhole, Indiana, and the Gray

Fossil Site, Tennessee (USA). *Palaeobiodiversity and Palaeoenvironments.* 96(2):239-254.

Palmeirim JM, Hoffmann RS. 1983. Galemys pyrenaicus. *Mammalian Species*, (207), 1-5.

Parmalee PW, Klippel WE, Meylan PA, Holman JA. 2002. A late Miocene-early Pliocene population of Trachemys (Testundines: Emydidae) from east Tennessee. *Annals Carnegie Museum*. 71:233–239.

Petersen KE, Yates TL. 1980. Condylura cristata. *Mammalian Species*, (129), 1-4.

Piras P, Sansalone G, Teresi L, Kotsakis T, Colangelo P, Loy A. 2012. Testing convergent and parallel adaptations in talpids humeral mechanical performance by means of geometric morphometrics and finite element analysis. *Journal of Morphology*, 273(7), 696-711.

Polly PD. 2007. Limbs in mammalian evolution. Chapter 15, pp. 245-268, in *Fins into Limbs: Evolution, Development, and Transformation*, Brian K Hall (ed.). University of Chicago Press: Chicago. (in press).

Reed CA. 1951. Locomotion and appendicular anatomy in three soricoid insectivores. *American Midland Naturalist*, 513-671.

Rohlf FJ. 2006. TPS software series. Department of Ecology and Evolution, State University of New York, Stony Brook.

Rohlf FJ, Loy A, Corti M. 1996. Morphometric analysis of Old World Talpidae (Mammalia, Insectivora) using partial-warp scores. *Systematic Biology*, 45(3), 344-362.

Rümke CG. 1985. *A review of fossil and recent Desmaninae (Talpidae, Insectivora)* (Doctoral dissertation, Utrecht University).

Rzebik-Kowalska B. 2014. Review of the Pliocene and Pleistocene Talpidae (Soricomorpha, Mammalia) of Poland. *Palaeontologia Electronica*, *17*(2), 1-26.

Saban R. 1958. Palaeanodonta. In Grassé, P. -P. (ed.), Traité de Paléontologie 6(2):521-533, Paris, Masson et Cie.

Sánchez-Villagra MR., Menke, P. R., & Geisler, J. H. 2004. Patterns of evolutionary transformation in the humerus of moles (Talpidae, Mammalia): a character analysis. *Mammal Study*, *29*(2), 163-170.

Sánchez-Villagra MR, Horovitz I, Motokawa M. 2006. A comprehensive morphological analysis of talpid moles (Mammalia) phylogenetic relationships. *Cladistics*, 22(1), 59-88.

Sansalone G, Kotsakis T, Piras P. 2015. Talpa fossilis or Talpa europaea? Using geometric morphometrics and allometric trajectories of humeral moles remains from Hungary to answer a taxonomic debate. *Palaeontologia Electronica*, 18(2), 1-17.

Schreuder A. 1940. A revision of the fossil water-moles (Desmaninae). *Archives néerlandaises de zoologie*, *4*(2), 201-333.

Schneider CA, Rasband WS, Eliceiri KW. 2012. NIH Image to ImageJ: 25 years of image analysis, *Nature methods* 9(7): 671-675.

Schwermann AH, Thompson RS. 2015. Extraordinarily preserved talpids (Mammalia, Lipotyphla) and the evolution of fossoriality. *Journal of Vertebrate Paleontology*. 35:e934828.

Sher A. 1999. Traffic lights at the Beringian crossroads. *Nature*, *397*(6715), 103.

Shinohara A, Campbell KL, Suzuki H. 2003. Molecular phylogenetic relationships of moles, shrew moles, and desmans from the new and old worlds. *Molecular Phylogenetics and Evolution*, *27*(2), 247-258.

Shinohara A, Suzuki H, Tsuchiya K, Zhang YP, Luo J, Jiang XL, Wang YX, Campbell KL. 2004. Evolution and biogeography of talpid moles from continental East Asia and the Japanese Islands inferred from mitochondrial and nuclear gene sequences. *Zoological science*, *21*(12), 1177-1185.

Shunk AJ, Driese SG, Clark GM. 2006. Latest Miocene to earliest Pliocene sedimentation and climate record derived from paleosinkhole fill deposits, Gray Fossil Site, northeastern Tennessee, USA. *Palaeogeography, Palaeoclimatology, Palaeoecology*, *231*(3-4), 265-278.

Shunk AJ, Driese SG, Dunbar JA. 2009. Late Tertiary paleoclimatic interpretation from lacustrine rhythmites in the Gray Fossil Site, northeastern Tennessee, USA. *Journal of Paleolimnology* 42:11-24.

Skoczeń S. 1980. Scaptonychini Van Valen, 1967, Urotrichini and Scalopini Dobson, 1883 (Insectivora, Mammalia) in the Pliocene and Pleistocene of Poland. *Acta zoologica cracoviensia*, *24*, 411-448.

Skoczeń S. 1993. New records of Parascalops, Neurotrichus and Condylura (Talpinae, Insectivora) from the Pliocene of Poland. *Acta Theriologica*, *38*(2), 125-137.

Smith AT, Xie Y. 2008. *A Guide to the Mammals of China*. Princeton University Press, Princeton, New Jersey.

Storch G, Qiu Z. 1983. The Neogene mammalian faunas of Ertemte and Harr Obo in Inner Mongolia (Nei Mongol), China. 2. Moles-Insectivora: Talpidae. *Senckenbergiana lethaea*, 64(2/4), 89-127.

Storch G, Qiu Z. 1991. Insectivores (Mammalia: Erinaceidae, Soricidae, Talpidae) from the Lufeng hominoid locality, Late Miocene of China. *Geobios*, *24*(5), 601-621.

Symonds MR. 2005. Phylogeny and life histories of the 'Insectivora': controversies and consequences. *Biological Reviews*, 80(1), 93-128.

Thewissen JGM, Badoux DM. 1986. The descriptive and functional myology of the fore-limb of the aardvark (*Orycteropus afer*, Pallas 1766). *Anat Anz*, *162*, 109-123.

True FW. 1896. *A revision of the American moles* (Vol. 19). US Government Printing Office.

Van den Hoek Ostende LW, Fejfar O. 2006. Erinaceidae and Talpidae (Erinaceomorpha, Soricomorpha, Mammalia) from the Lower Miocene of Merkur-Nord (Czech Republic, MN 3). *Beiträge zur Paläontologie*, *30*, 175-203.

Vila R, Bell CD, Macniven R, Goldman-Huertas B, Ree RH, Marshall CR, Pierce NE. 2011. Phylogeny and palaeoecology of Polyommatus blue butterflies show Beringia was a climate-regulated gateway to the New World. *Proceedings of the Royal Society of London B: Biological Sciences*, *278*(1719), 2737-2744.

Wallace SC, Wang X. 2004. Two new carnivores from an unusual late Tertiary forest biota in eastern North America. *Nature*, *431*(7008), 556.

Whidden HP. 2000. Comparative myology of moles and the phylogeny of the Talpidae (Mammalia, Lipotyphla). *American Museum Novitates*, 1-53.

Whitelaw JL, Mickus K, Whitelaw MJ, Nave J. 2008. High-resolution gravity study of the Gray Fossil Site. *Geophysics*, *73*(2), B25-B32.

Wolfe JA. 1975. Some aspects of plant geography of the Northern Hemisphere during the late Cretaceous and Tertiary. *Annals of the Missouri Botanical Garden*, 264-279.

Worobiec E, Liu Y, Zavada MS. 2013. Palaeoenvironment of late Neogene lacustrine sediments at the Gray Fossil Site, Tennessee, U.S.A. *Annales Societatis Geologorum Poloniae*. 83:51-63.

Yalden DW. 1966. The anatomy of mole locomotion. *Journal of Zoology*, *149*(1), 55-64.

Yates TL. 1984. Insectivores, elephant shrews, tree shrews and dermopterans. In: Anderson S, Jones JK, Jr., editors. Orders and families of recent mammals of the world. New York: Wiley. p. 117–144.

Yates TL, Moore DW. 1990. Speciation and evolution in the family Talpidae (Mammalia: Insectivora). *Prog Clin Biol Res*. 335:1–22.

Ziegler R. 2003. Moles (Talpidae) from the late Middle Miocene of South Germany. Acta *Palaeontologica Polonica* 48:617–648.

Ziegler R. 2012. Moles (Talpidae, Mammalia) from Early Oligocene karstic fissure fillings in South Germany. *Geobios* 45:501–513.

Zobaa MK, Zavada MS, Whitelaw MJ, Shunk AJ, Oboh-Ikuenobe FE. 2011. Palynology and palynofacies analyses of the Gray Fossil Site, eastern Tennessee: Their role in understanding the basin-fill history. *Palaeogeography, Palaeoclimatology, Palaeoecology*, *308*(3-4), 433-444.

VITA

DANIELLE E. OBERG

Education:	B.S., Geological Sciences (Honors), University of Oregon (UO), Eugene, OR, 2015 M.S., Geosciences, East Tennessee State University (ETSU), Johnson City, TN, 2018
Professional Experience:	Research Assistant, University of Oregon Department of Geological Sciences, Eugene, OR, 2014 – 2015 Robotics and 3D Printing Summer Camp Instructor, Eugene Sudbury School, Eugene, OR, 2015 Collections Assistant, University of Oregon Museum of Natural and Cultural History, Eugene, OR, 2014 – 2016 Graduate Research Assistant, East Tennessee State University, Johnson City, TN, 2016 – 2017 Tutor, East Tennessee State University, Johnson City, TN, 2016 – 2018 Field Assistant, Don Sundquist Center for Excellence in Paleontology, Gray, TN, 2017 Graduate Collections Assistant, Don Sundquist Center for Excellence in Paleontology, Gray, TN, 2017 – 2018
Publications (in preparation):	Oberg, D. E. and Hopkins, S. S. B. (2018). Eulipotyphlans from the Mascall Formation, OR. (in preparation for *Paleoelectronica*) Oberg, D. E. and Hopkins, S. S. B. (2018). New marsupial occurrence in Oregon's Middle Miocene. (in preparation for *Journal of Vertebrate Paleontology*) Oberg, D. E., Famoso, N. A., and Hopkins, S. S. B. (2019). Reconstructing body mass from marsupial dental measurements. (early stage)
Awards and Honors:	ROTC Dean's Scholarship Maintaining high GPA while being full-time student and full-time ROTC cadet, University of Oregon Outstanding Student Employee Nominated by academic department for outstanding student work, University of Oregon UO Department of Geological Sciences Field Camp Scholarship Scholarship to cover the cost of attending UO geological sciences' field camp program, University of Oregon UO Dean's List GPA above 3.75 for semester, University of Oregon